CHESS Lab Bulletin

2018

Vol.1 No.2

CHESS Lab

Coastal Hazards and Energy System Science Lab
Graduate School for International Development and Cooperation (IDEC)
Hiroshima University

Contents

CHESS Lab members

Han Soo Lee: Associate Professor

- **Email**: leehs(at)hiroshima-u.ac.jp
- **Research subject**: Coastal engineering
- **Research interests:** storm surge, tsunami, wind waves, typhoons, coastal hazard risk analysis, sustainable energy strategy in developing countries, time series analysis

Guiamel Ismail Adal (M2)

- **Research topic:** Access to Quality Waters and Energy in Mindanao, Philippines
- **Research interests:** Renewable energy, safe water

Md Morshed Bin Shiraj (M2)

- **Research topic:** Storm surge and flood
- **Research interests:** Natural Disasters, Mathematical Modeling, Astronomy, Robotics, Mathematical Analysis, etc

Alex Bunodiere (M1)

- **Research topic:** Renewable energy curtailment in Japan
- **Research interests:** Renewable energy (Solar and wind energy, …) and Sustainable development

Mochamad Riam Badriana (M1)

- **Research topic:** Multi-model ensemble projection of future wave climate in the western North Pacific using CMIP5 dataset
- **Research interests:** Coastal Current, Waves, Oceanographic modelling

Wirawan Widiyanto (M2)

- **Research topic:** Identifying Indonesia's Key Factors for Pre-Disaster Recovery Plan
- **Research interests:** Disaster Management

Hort Seng (M1)

- **Research topic:** Control Renewable Energy and Smart Grid
- **Research interests:** Solar, Wind, and Hydropower plant

Mbalenhle Immaculate Shabalala (Research student)

- **Research topic:** Simulation and Management of Solar Photovoltaic Power Plants Supply in Rural KwaZulu Natal with Smart Metering
- **Research interests:** Renewable energy, distributed generation, smart grid

---

Ricard Diago Sambuaga (Research student)

- **Research topic:** Optimized Evacuation Plan and Decision Support System Development with Agent-Based Modeling (ABM) for Earthquake and Tsunami in Palu, Indonesia
- **Research interests:** Agent-Based Modeling, Tsunami, Evacuation Plan and System

---

Wahidullah Hussainzada (Research student)

- **Research topic:** Sustainable Water Research Management on Balkh River Basin
- **Research interests:** IWRM

Kotaro NAKATSUKA (B4)

- **Research topic:** CMIP5 データ解析による日本における風力エネルギー資源の将来予測
- **Research interests:** Renewable energy; wind energy

Yukiya KOJIMA (B4)

- **Research topic:** 波浪中を低速航行する船舶に働く流体力と運動に関する研究
- **Research interests:** mooring; renewable energy; offshore wind power

---

Thomas Hocking （University of Graz）

- **Research topic:** TBD
- **Research interests:** Earth system modeling, atmospheric science, renewable energy, sustainable development

---

Nicholas Denegre （University of Graz）

- **Research topic:** TBD
- **Research interests:** Photovoltaic systems, renewable energy grid integration, coral reef degradation

---

Vinayak Bhanage (D2)(Center of Studies in Resources Eng., IIT Bombay)

- **Research topic:** Impacts of UHI over Indian Cities
- **Research interests:** Urban Microclimate, Land surface processes, Aerosol radiative forcing and its impacts

Evaluation and Bias Correction of marine Surface Winds from CMIP5 GCMS for wave climate modelling in the Western North Pacific

Mochamad Riam Badriana[1]

[1]Graduate School for International Development and Cooperation, Hiroshima university, 1-5-1 kagamiyama, Higashi-Hiroshima 739-8592, Hiroshima, Japan

Abstract

Wind waves play important roles in coastal and oceanic hazards, and sea environment. The western Northern Pacific (WNP) is commonly indicated as region with high occurrence of high waves due to typhoons for decades. The increasing trend of typhoon frequency and intensity can be observed through general circulation models (GCMs) output, in example CMIP5. CMIP5 consist of a set of ensemble data including the marine surface winds for future wave climate modelling. Therefore, surface winds from CMIP5 GCMs and their validations to reference data are essential to inspect their quality and uncertainty for wind wave modelling. In this study, we investigate the bias in marine surface winds from CMIP5 GCMs over the WNP. The monthly surface winds from ERA-Interim reanalysis data and MRI-CGCM3 in CMIP5 for thirty years from 1979 to 2009 is taken account as reference data and model data, respectively. Over the WNP region (110 – 170ºE and 10 – 60ºN), the time series of reference and modelled grid-point marine surface winds at every 10 deg in longitude and 5 deg in latitude are investigated to find out their correlations. Then bias correction method using a linear regression is proposed to reduce the bias in marine surface winds. The time series of surface winds at grids are also investigated and show seasonal and annual patterns correlated with Pacific Decadal Oscillation (PDO) and Western Pacific (WP) indices. Several points depict good agreements between reference and model data located on southwestern and northeastern parts of the study domain, but correlations between seasonal indices are still unclear. The proposed bias correction method in this study exhibits good improvement of the modelled marine surface winds for the study period in the WNP. In further study, the seasonal and annual patterns and correlations with indices in addition to the bias correction method will be used to improve the future marine surface winds from CMIP5 GCMs for future wave climate modeling.

Keywords: bias correction, ERA-Interim, MRI-CGCM3, linear regression, CMIP5, the western North Pacific

1. Introduction

Future changes in surface wind have implication for ocean-atmosphere phenomenon, particularly wind waves, storm surges and typhoons. The increasing trend of emission and sea-level rise is evidence for a possibility of different wind behavior in the following decades. CMIP5 provides several scenarios for historical and future condition adopted by IPCC Assessment Report (AR5).

CMIP5 data have more comprehensive and better documentation other than previous phases. Through gateways to modeling and data centers worldwide, the dataset could be archived freely (Taylor et al., 2012). Many researchers dealing CMIP5 data for ocean-atmospheric modeling. Shimura et al. (2013) used CMIP5 to predict wave climate pattern and compare with teleconnection pattern index, Hemer et al. (2013) calculated wave parameter in summer and winter use multi-model ensemble, Bennet et al. (2016) observed future wave climate in UK sea, and Shimura et al (2016) found the future decreases in wave heights correspond to positive changes in the WP pattern using CMIP5 scenario.

The reliability of ocean-atmospheric modeling depends on the quality of wind data itself. Since wind is the source which generates wind waves, the improper wind data will produce low quality of output model. Furthermore, it will lead to incorrect analysis and comprehension in using provided CMIP5 data. A good agreement in validation is necessary to convince the utility of ensemble data, otherwise it will be just random model with more uncertainty.

MRI-CGCM3 has finest resolution among other ensembles with almost 150km resolution for each longitudinal and latitudinal grid. Fine resolution dataset commonly has close value with observation since it obtains more detailed obstacle information which can affect most of wind data. It is expected that MRI-CGCM3 has good agreement compare to another CMIP5 model. However, verification between model and data is necessary to be done. The difference from both data resulted bias which inevitable as uncertainty factor in ensembles. To narrow the vast possibility of future condition, the uncertainty must be avoided as many as possible.

Bias correction over the West Northern Pacific (WNP) applied to reduce error between model and reanalysis dataset. The correction can be reduced with many methods. We propose linear regression in reducing the bias in marine surface winds. The time series of surface winds at grids are also investigated and show seasonal and annual patterns correlated with Pacific Decadal Oscillation (PDO) and Western Pacific (WP) indices. In further study, the seasonal and annual patterns and correlations with indices in addition to the bias correction method will be used to improve the future marine surface winds from CMIP5 GCMs for future wave climate modeling

2. Objectives

CMIP5 data consist many kind data that can be useful for environmental modeling and analysist. However due to uncertainty of many ensemble models provided, validation is necessary. There is increasing study in term of wind wave. Some study done by Hemer et al. (2013) and Bennet et al. (2016) which correlated significant wave height between ensembles and satellite data or observation measurement. Those study applied wind from coupled general circulation model (GCMs) to ocean model to obtain the wave height. In other words, the quality of produced wind wave depends on wind input. Consequently, each ensemble wind needs to be observed further.

This study seeks the agreement of MRI-CGCM3 model as the finest spatial resolution model among CMIP5 ensembles. we derive historical data of wind surface which is obtained between 1979 and 2008. This study stands as preliminary study before using any CMIP5 wind surface ensemble data for wind wave, cyclone, and another atmospheric-ocean event. Model data will be observed using simple statistical approach and be compared with reanalysis data.

3. Data and methodology

3.1 Data

An independent intergovernmental organization which is supported by 34 states developed European Centre for Medium-Range Weather Forecast (ECMWF). It provides global reanalysis and numerous meteorological data until present time in their public dataset. Monthly data from ERA-Interim is chosen over 30 years from 1979 to 2008. The resolution is 0.75^0 x 0.75^0 but to simplify the comparison, we do interpolation for 1 degree. Then, this data treated as reference data.

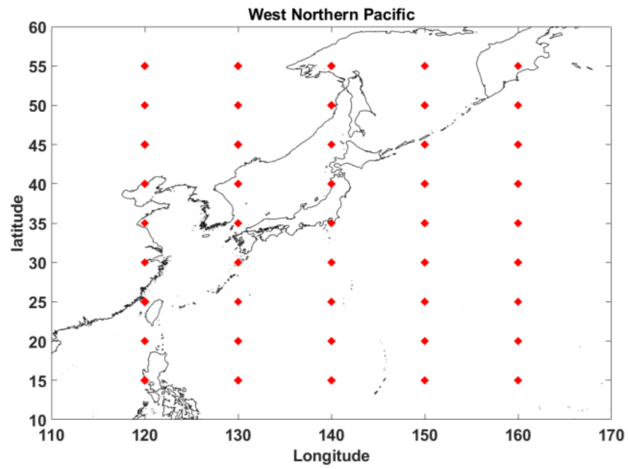

Figure 1. Location of observed point

Ensemble data (Table 1) has similar length of data (around 30 years) but the resolution of each ensemble is different. The Experiment of AMIP is chosen. Historical data in CMIP5 database includes changing conditions of atmospheric composition (anthropogenic and volcanic influence), solar forcing, emission, and land use. In AMIP experiment, sea surface temperature & sea ice (from observations) are imposed in addition to historical experiment (Taylor et al., 2009). Ensemble variances in one GCM model indicates the different initial condition, parameterization, and physical parameter. In this study, MRI-CGCM3 is chosen for its resolution among the others. Most of the data do not overlap with reanalysis grid point, thus simple interpolation of 1 degree is elected as the representative ensemble. The monthly average of *u* and *v* component of surface wind are retrieved.

Table 1. Model ensemble resolution. Number inside bracket indicates the total model ensemble

Model ensemble	Resolution	
	Latitude	Longitude
ACCESS1.0 ACCESS1.3 (ii)	1.25^0	1.875^0
INM-CM4	1.5^0	2^0
GFDL-CM3 (ii)	2^0	2.5^0
CNRM-CM5	1.4008^0	1.40625^0
CanAM4 (iv) MIROC-ESM	1.7906^0	2.8125^0
IPSL-CM5A-LR	1.8947^0	3.75^0
IPSL-CM5A-MR	1.2676^0	2.5^0
MRI-CGCM3	1.121^0	1.125^0
GISS-E2-R (ii)	2^0	2.5^0

3.2 Methodology

Both of model and reference data consists wind component of *u* and *v* (above surface at 10-m height). To be compared well, each ensemble's wind component is simply calculated to find wind magnitude. Using simple statistical approach as maximum, minimum, and mean can discovered the uncertainty of ensemble data. Thus, correlation and standard deviation of each ensemble can be obtained. Wind trend is observed to see the changing pattern from past to current. simple subtraction between both datasets is shown as bias in 2D map over WNP region.

EOF

We first propose Empirical Orthogonal Function (EOF) to observe the pattern and to reduce bias by its spatial pattern over WNP region. EOF analysis is often used to study possible spatial modes (patterns) of variability and how they change with time. Classified as multivariate statistical technique, it interprets each individual pattern has physical / dynamical meaning. EOF are found by computing the eigenvalues and eigenvectors of a spatially weighted anomaly covariance matrix of a field. However, there is no priori hypothesis based on probability distribution and statistical test yet. We hope the bias can be corrected with subtraction between model data and each produced mode.

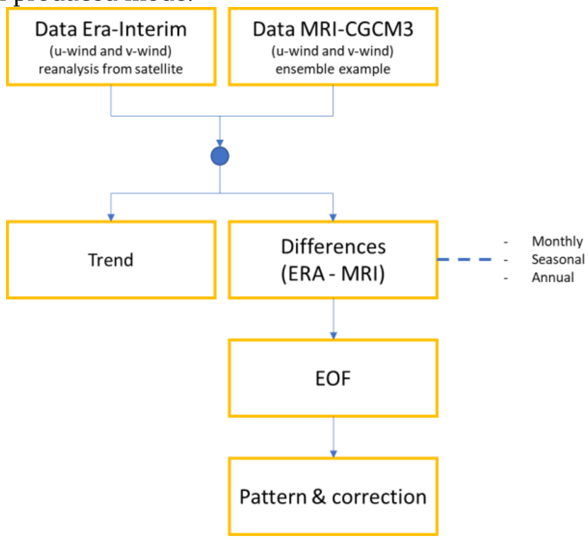

Figure 2. Research methodology structure

Bias correction

Common wind data can be underestimated or overestimated compare to reference data. The differences between them caused by several factor, particularly different initial condition, parameter configuration, existed obstacle and typhoon, quality of data, surface roughness, and model resolution. Simple linear regression is used to reduce the uncertainty. Each observation point has linear trend between reanalysis and model, thus correcting the trend coefficient is expected to give less error.

4. Results

Wind timeseries for whole 30 years of MRI-CGCM3 data tends to have similar pattern with reanalysis timeseries. The value of bias, R^2, and root mean square error (RMSE) had been calculated. Some point had good value indicates good agreement between model and reference, in example on 120^0E and 20^0N (Figure 3). Almost each grid has similar pattern and phase of timeseries, even the bias is still large. The R^2 is around 0.1 – 0.65, while the bias around ±2.8 m/s.

Average wind speed of 30 years is plotted in 2D map. The difference between model & reference is shown in Figure 4. Winter exhibits stronger wind speed than another season. In average winter season, strong wind appeared in 10^0-20^0 N and 30^0-45^0N. In the following season of spring and summer, the windspeed pattern shifted to the equator while it shifted back to northern hemisphere on autumn season. Reference and model pattern give similar pattern, however in some part the difference is high. The white color in differences map show less bias that can be neglected. Red region indicates the reference data is higher than model, while blue region shows the model is underestimate.

Linear trend of model and reference data series showed small increasing / decreasing trend in each point. Reference data is dominated by decreasing trend while most of model data has increasing trend on its observation point. Small value close to 0 can be assumed no significant change of windspeed pattern for over 30 years. Otherwise, the fluctuation between positive and negative value has similar range made the trend look like constant line. The trend is around ±2.5 x 10^{-3}.

EOF produced around 80 modes that contribute to two-dimensional bias pattern. Figure 6 shows the

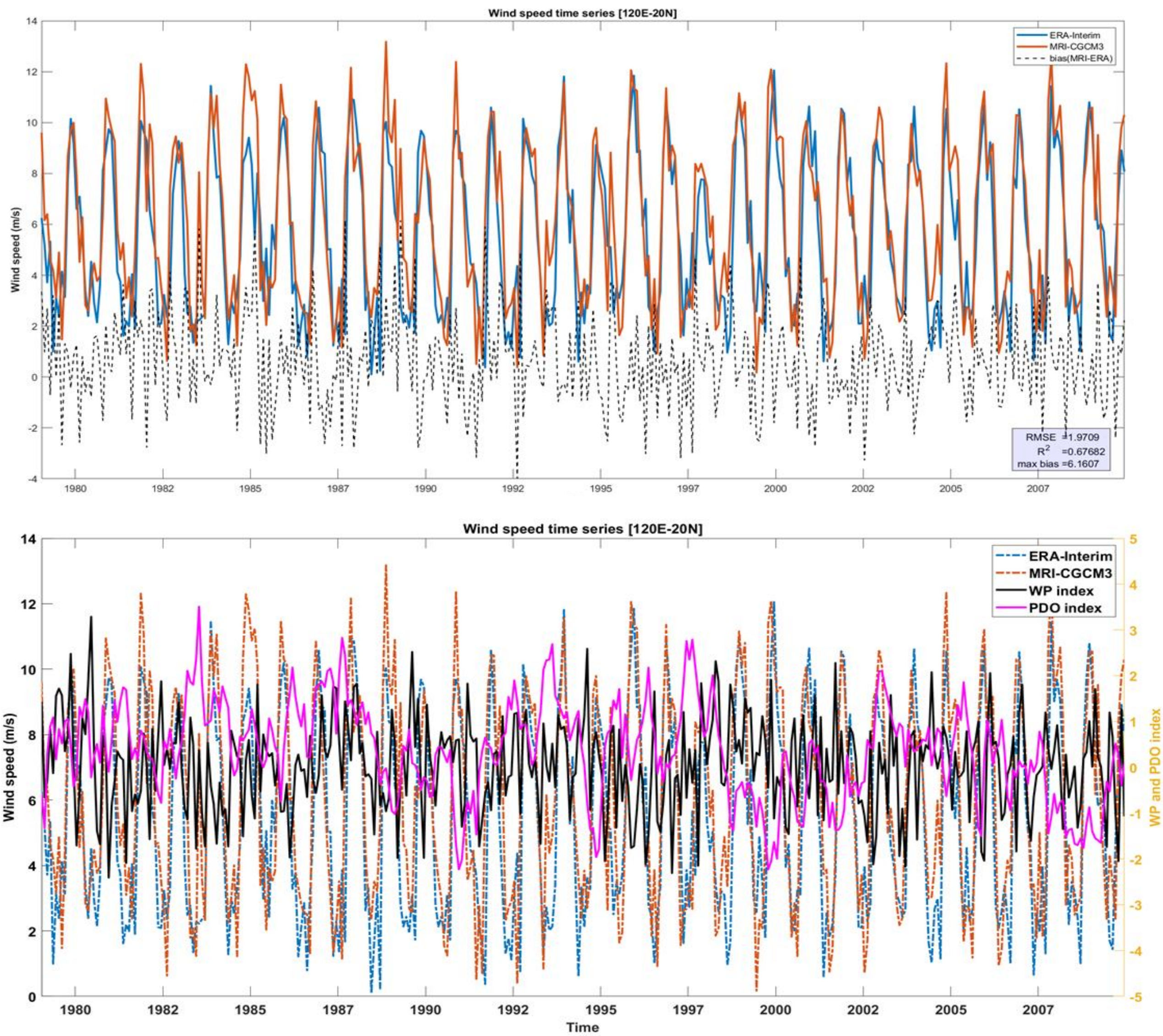

Figure 3. Time series of reference and model data on specific point and compare with WP and DPO index.

resulted EOF from bias between two data in winter season. The pattern can be divided as positive and negative contribution. However, the value is small compare to bias pattern. It is expected to have similar pattern if all modes are combined. However, the value is too small than the raw bias.

The index of DPO and WP pattern had been compared with ensemble time series. However, it is not trivial to see the index relation with monthly and seasonal moving average. However, if the DPO index is adjusted with yearly moving average. wind timeseries, there are certain periods which have relation with the index. For a moment, we cannot pronounce the relation between index and wind surface time series.

5. Discussion and Limitation

The calculation of bias correction s still limited due to matter of comprehensive method. Dealing correction with linear regression is not a simple as it is. Statistically, the bias will be corrected, but the wind data series will be changed overall. If we only shift the windspeed trend, certain point could have less error while other points have larger error.

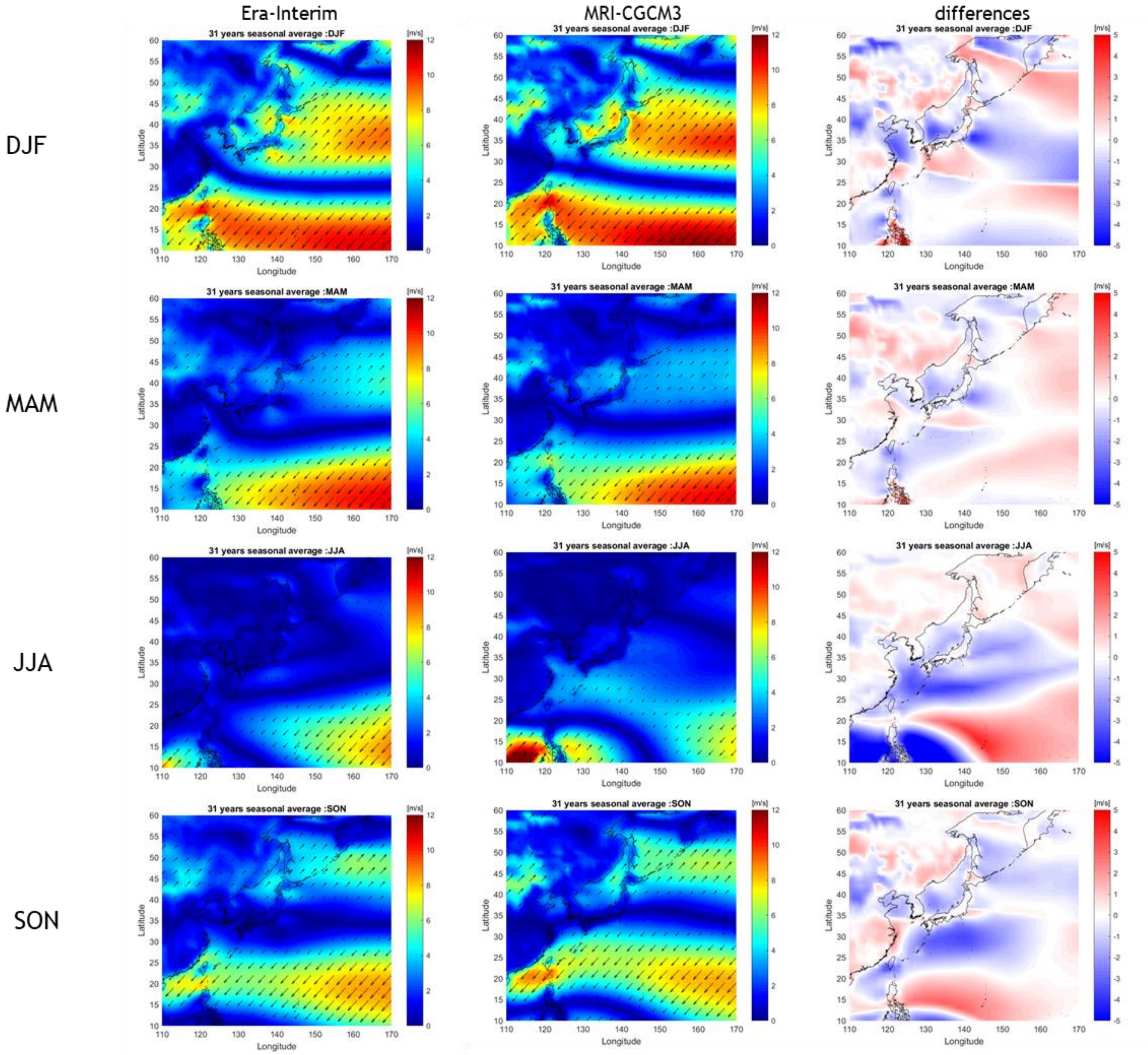

Figure 4. Average of 30 years windspeed over WNP region for ERA-Interim (left), MRI-CGCM3 (middle), and model differences (right)

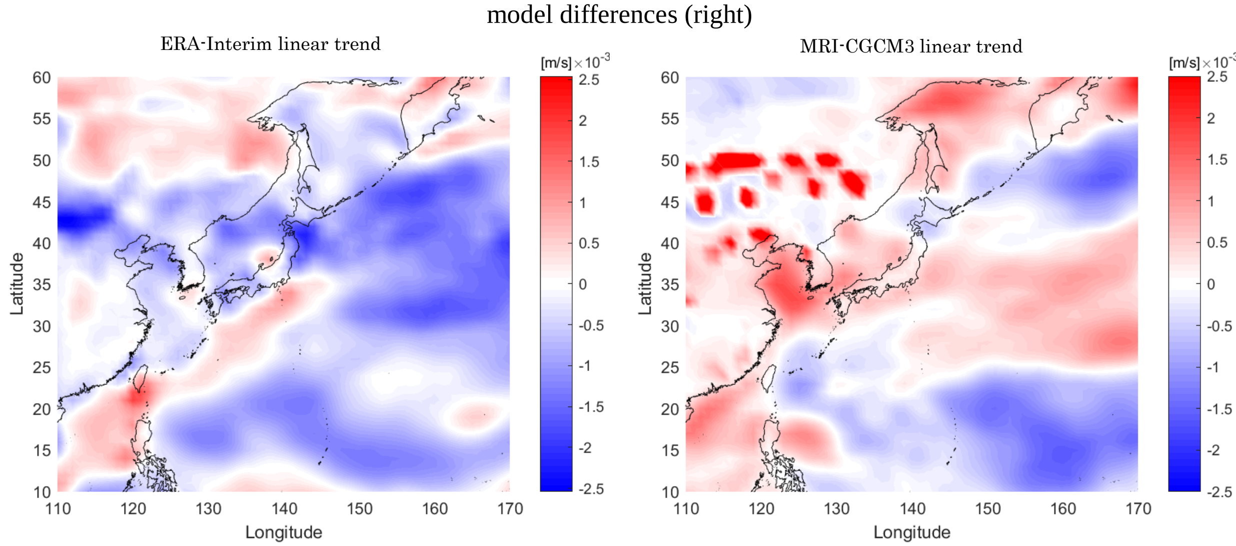

Figure 5. Linear trend between reference (left) and model data (right) over WNP region.

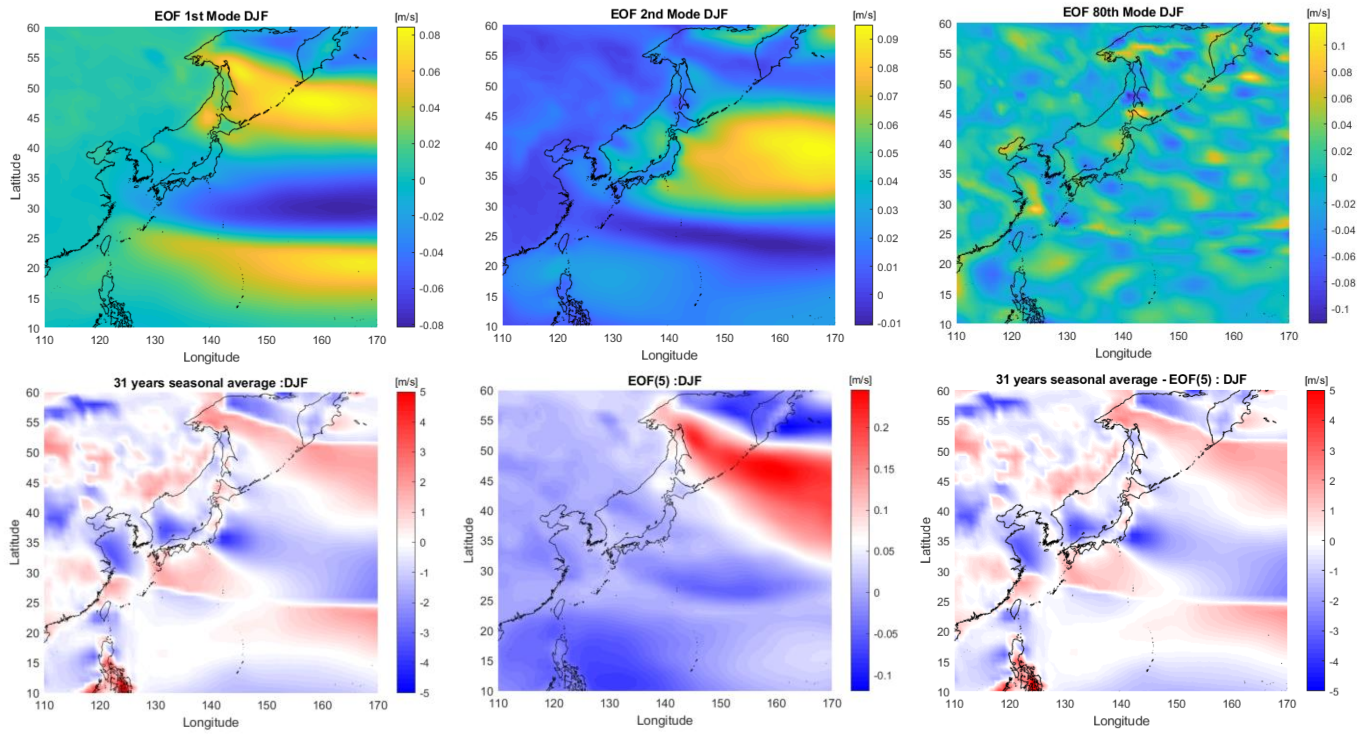

Figure 6. EOF from winter bias over WNP region. Upper part shows the 1st , 2nd and 80th (last mode) as resulted by EOF analysist. Lower part shows the reduction of bias after corrected with cumulative EOF mode (mode 1 – 5).

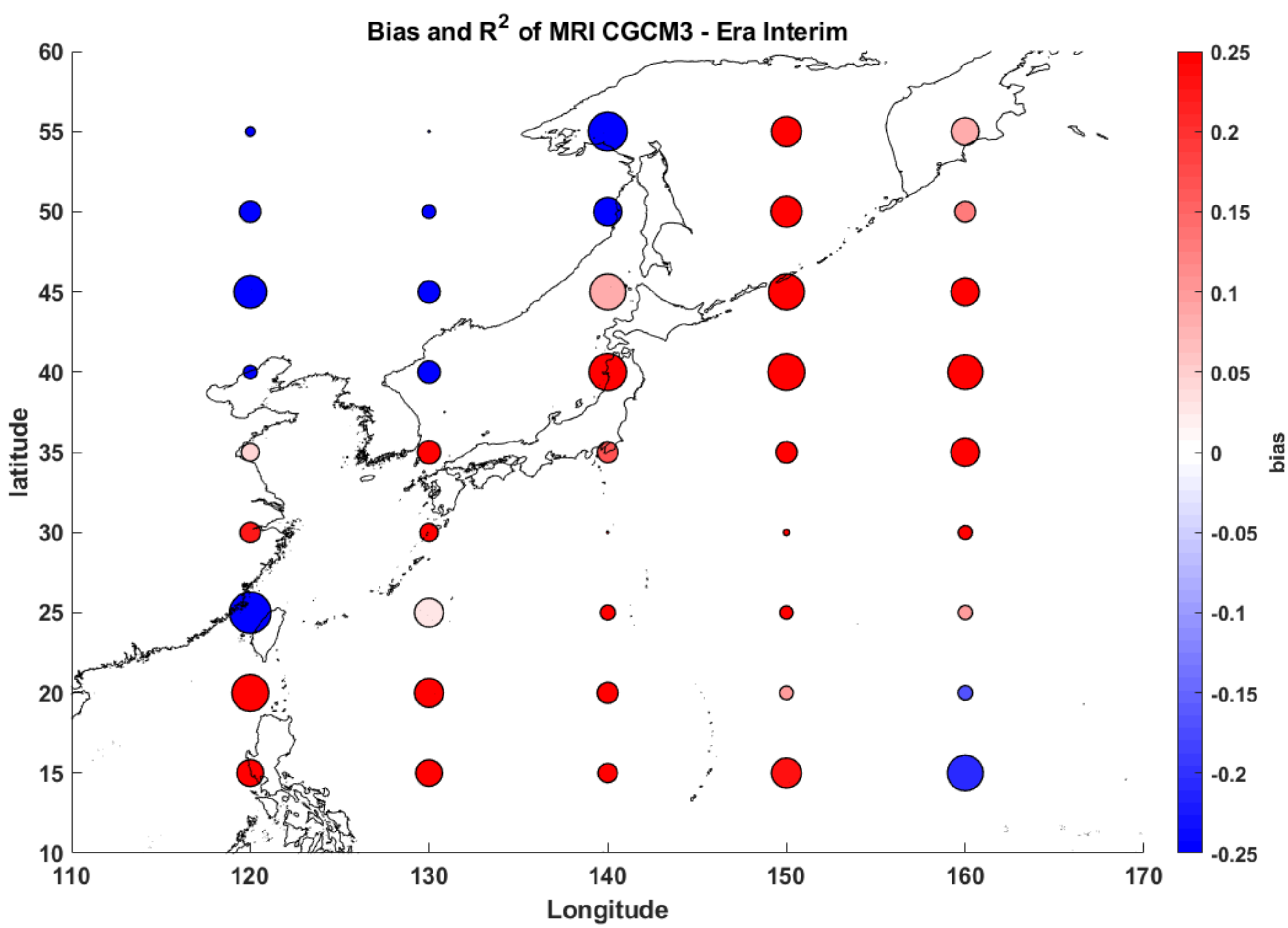

Figure 8. EOF from winter bias over WNP region. Upper part shows the 1st , 2nd and 80th (last mode) as resulted by EOF analysist. Lower part shows the reduction of bias after corrected with cumulative EOF mode (mode 1 – 5).

EOF produced around 80 modes that contribute to two-dimensional bias pattern. Theoretically, small number of modes has more contribution than the rest of the modes. However, merging all modes cannot reconstruct the pattern into bias pattern. It is assumed that EOF analysis result is not good caused by script error or misinterpretation. Also, there is still problem faced using EOF, such as orthogonality, domain shape, and Buell patterns problem.

6. Things to be done further

MRI-CGCM3 and ERA-Interim show good agreement in several point. However, the bias in the location which have high R^2 also have large bias. Other clear and effective method for bias correction is still needed. Linear trend can be inspected also using many methods, thus for further study, EMD, EEMD, etc. method will be applied.

Carry out the future scenario of CMIP5 and wind input modeling is not part of this study but it can be next step for upcoming study. The newest CMIP6 also have potential for advanced research.

References

Bennett, W., Karunarathna, H., Mori, N., & Reeve, D. (2016). Climate Change Impacts on Future Wave Climate around the UK. *Journal of Marine Science and Engineering*, *4*(4), 78. https://doi.org/10.3390/jmse4040078

Hemer, M. A., Fan, Y., Mori, N., Semedo, A., & Wang, X. L. (2013). Projected changes in wave climate from a multi-model ensemble. *Nature Climate Change*, *3*(5), 471–476. https://doi.org/10.1038/nclimate1791

Holmes, J. D. (2015). *Wind loading of structures* (3rd ed). CRC. Retrieved from http://ci.nii.ac.jp/ncid/BB19758031.bib

Shimura, T., Mori, N., & Mase, H. (2013). Ocean waves and teleconnection patterns in the northern hemisphere. *Journal of Climate*, *26*(21), 8654–8670. https://doi.org/10.1175/JCLI-D-12-00397.1

Shimura, T., Mori, N., & Hemer, M. A. (2016). Variability and future decreases in winter wave heights in the Western North Pacific. *Geophysical Research Letters*, *43*(6), 2716–2722. https://doi.org/10.1002/2016GL067924

Taylor, K. E., Stouffer, R. J., & Meehl, G. a. (2007). A Summary of the CMIP5 Experiment Design. *World*, *4*(January 2011), 1–33. https://doi.org/10.1175/BAMS-D-11-00094.1

USING THE SOIL AND WATER ASSESSMENT TOOL (SWAT) TO SIMULATE THE WATERSHEDS OF MINDANAO BASINS FOR HYDROPOWER ENERGY DEVELOPMENT

Guiamel, Ismail Adal
Master's Student, Graduate School of International Development Cooperation, Hiroshima University

Author's Note

This paper was written by Mr. Guiamel, a master's student under Coastal Hazard Energy System Science in Development Technology. This paper is a summary of the research progress in the Autumn semester of 2019.

Contact information thru email address iguiamel@gmail.com and/or mobile number (+8) 80 9818 7009.

February 2019

Abstract

This study aims to simulate the watershed for the estimation of theoretical potential hydropower energy in the Mindanao River Basin (MRB) of the Philippines. The country has total 18 major river basins and the MRB is the second largest river basin in the Philippines with a total area of 21,503 square kilometer that covers 7 provinces, 72 municipalities and 1,731 barangays (villages). The Buayan Basin is the eighteenth largest river basin in the country with an area of 1,435 square kilometers situated in the Southern part of Mindanao Region. Despite these resources, the region is still facing challenges on the power shortage due to increasing demand with an average growth rate of approximately 3.8 % in the past decades. Last April 2017 the maximum peak demand reached about 1,696 MW. Therefore, in order to strengthen the supports to government policy to accelerate the exploration of the resources for the renewable energy in accordance to the Renewable Act of 2008 of the Philippine the authors conduct watershed modeling to assess the theoretical hydropower potential using ArcSWAT interface in Geographic Information System (GIS). SWAT modeling and the interfaces could help to address the budget-constrained for the assessment of hydropower potential of the watersheds. The inputs for the hydrological modeling are Synthetic Aperture Radar - Digital Elevation Model (SAR-DEM, 10m resolution), land use, soil type and weather datasets such as precipitation, wind speed, solar radiation, temperature, and humidity. Moreover, the precipitation datasets were carefully examined by comparing multi-global gridded and observed datasets at General Santos station. The correlation of the monthly precipitations from observes station (DOST-PAGASA)[1] are 0.78 for GPCC[2], 0.75 for NCDC-GSOD [3] and 0.43 for NCDC-CPC[4]. The model simulates the rivers discharges of multiple watersheds of Major basins. Then, it is calibrated using SWAT-CUP[5] to validate from the observed river discharges at Buayan River and other selected river gauges in Mindanao River basin. Subsequently, the theoretical hydropower potential is computed using the terrain analysis algorithm and discharge calculation from the water head. Finally, the results of this study will support the authorities, policy maker and investors for the watershed development and setting up hydropower in Mindanao Region of the Philippines.

Keywords: SWAT, Mindanao River, Buayan River, discharge, hydropower, watershed modeling

1. Introduction

The Philippines is situated in Southeast Asia in the western rim of the Pacific Ocean with 7,107 Islands, total land area 300,000 square sq.km, and coastline of around 36,289. Islands were group into three major part such as Luzon, Visayas, and Mindanao with the land areas of 141,000 sq.km, 57,000 sq.km, and 102,000 sq.km respectively. It has 17 regions, 80 provinces, 138 cities, 1,496 municipalities and 42,025 barangays *(village-level administrative units).* Moreover, the Philippines has the total population of 100,981,437 with the density 330/sq.km [1]. In addition, there are four climate types as defined in the spatial distribution of monthly rainfall [2]. On the other hand, the Philippines power sector is divided into three major components such as power transmission, power generation, and power distribution were the National Power and Private operators are coexisting for the operations and management of energy resources and allocations.

Mindanao has a total population of 24,135,775[1], 97.530 total land area, six (6) regional administrative, 27 provinces, 35 cities and 422 municipalities, 8 major basins as shown in figure 1. Furthermore, Philippine has a total 18 major basin and the Mindanao basin is the second largest basin while the Buayan basin is the eighteen largest basins in the country. Figure 3 illustrates the comparison of the major basins in Mindanao as well as the watershed of the study site. Also from figure 3 presented the location of the meteorological agencies both observed and gridded datasets[2][3].

DOST-PAGASA[1]: Department of Science and Technology, Philippines Atmospheric Geophysical and Astronomical Services Administration

GPCC[2]: Global Precipitation Climatology Center

NCDC-GSOD[3]: National Climatic Data Center, Global Summary of the Day

NCDC-CPC[4]: National Climatic Data Center, Climate Predicted Center

SWAT-CUP[5]: SWAT- Is the acronyms for Soil and Water Assessment Tool, the SWAT-CUP is public domain program for calibration of the SWAT model.

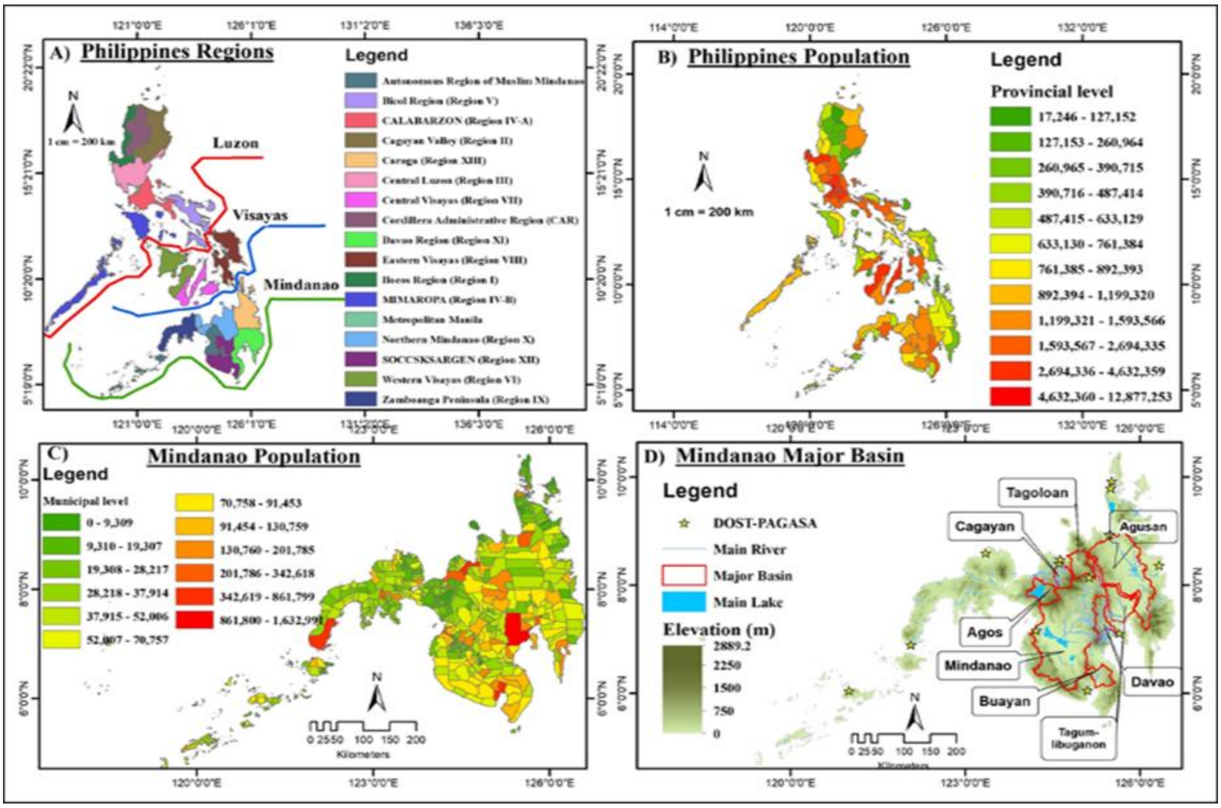

Figure 1: Basic information of the Study area; Philippines Population, Administrative, and Mindanao population including the major basins.

According to the Bangsamoro Development Plan, the Mindanao power demand has an increasing trend of 3.8 % in the past decades as per Department of Energy report. Last April 2017 the maximum peak demand reached about 1,696 MW. Moreover, the Department of Energy (DOE) stated in the report that the country's economy has been driven by the huge contribution of the power sectors. The total energy installed capacity of the country was increased from the level of 16,226.9 MW in 2011 to 17,025.0 megawatts (MW) in 2012, it is around 6 percent. Despite the development efforts of the power sector to improve the services and sustaining the electricity supplies to the consumers for the past years however the big challenge on increasing electricity demand continued with an annual average rate of 4.3 percent. In islands grid, the increasing demand is also remained a major challenge and there is no assurance to add more capacity. Consequently, to meet the domestic power demand, the power sector needs to add at least 13,166.7 MW[4]. As of June 2017, Mindanao has total gross power generation of 5,170,538 MWh; 7% geothermal, 7% oil based, 38% hydropower and 48% coal. Furthermore, the total installed capacity is 3,141MW and 2,717 MW dependable. The Generation capacity consists of coal 1070 MW, oil based 788 MW, geothermal 108, hydropower 1,080 MW, solar 59 MW and biomass 36 MW[5]. From these power capacity, 1,264 MW is the total renewable energy generated. Mindanao is consisting of "On-grid" and "Off-grid" and operated at the voltage class, there are 27 electric cooperatives in the region that connects to the transmission of 138kV and 69kV as shown in figure 2[6]. Bedside, the hydropower resources contributed 9.9 percent share to the total indigenous energy supply of the country and production played a significant increase of 21.7 percent, from 1.9 MTOE in 2010 to 2.4 MTOE due to the additional 91.0 MW capacity in 2011[4].

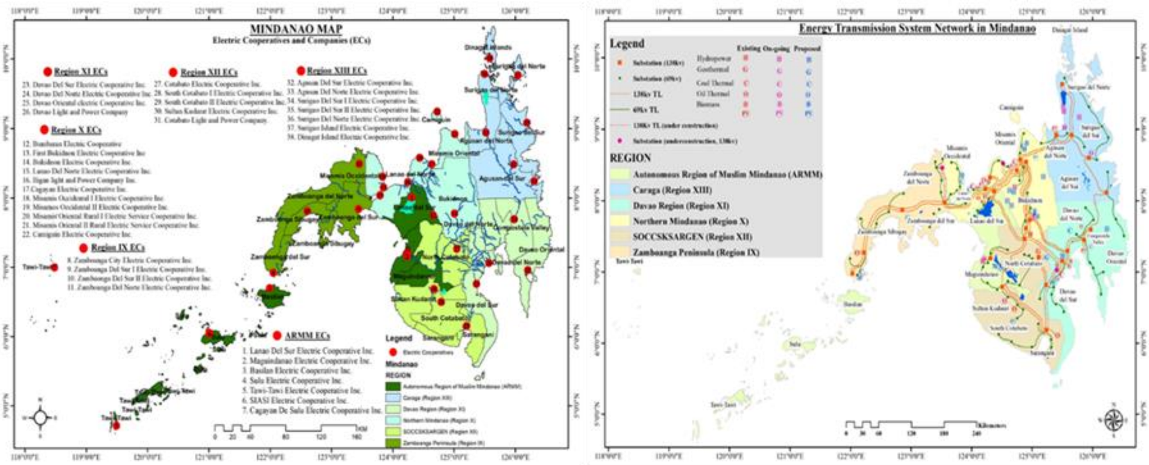

Figure 2: Map of the Electric companies and cooperatives, and its grid connection in Mindanao.

2. Study Area and Objectives

2.1. Study Site

This study basically focusses in the Mindanao major basins as shown in figure 2. The Mindanao River Basin (MRB) is the second largest river basin in the Philippines with a total area of 21,503 square kilometers as shown in figure 3. It covers seven provinces such as Maguindanao, Lanao del sur, Bukidnon, Sultan Kudarat, Davao del Norte, North Cotabato, and South Cotabato. MRB has 72 municipalities and 1,731 barangays[7]. While Buayan Basin is the eighteenth largest river basin in the country with an area of 1,435 square kilometers situated in the Southern part of Mindanao Region[8], see figure 3.

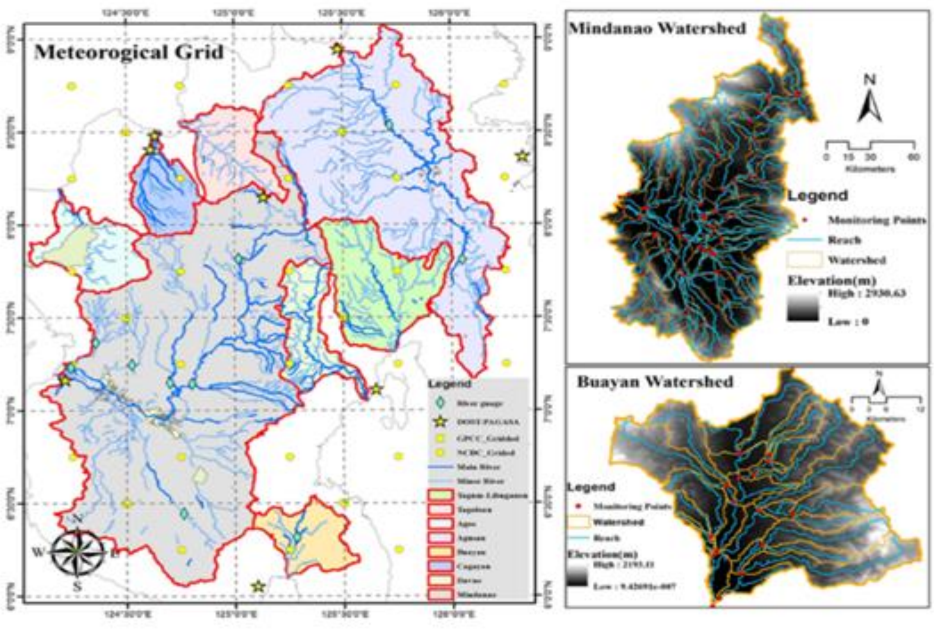

Figure 3: Meteoritical Agencies in the major basin of Mindanao, a watershed for

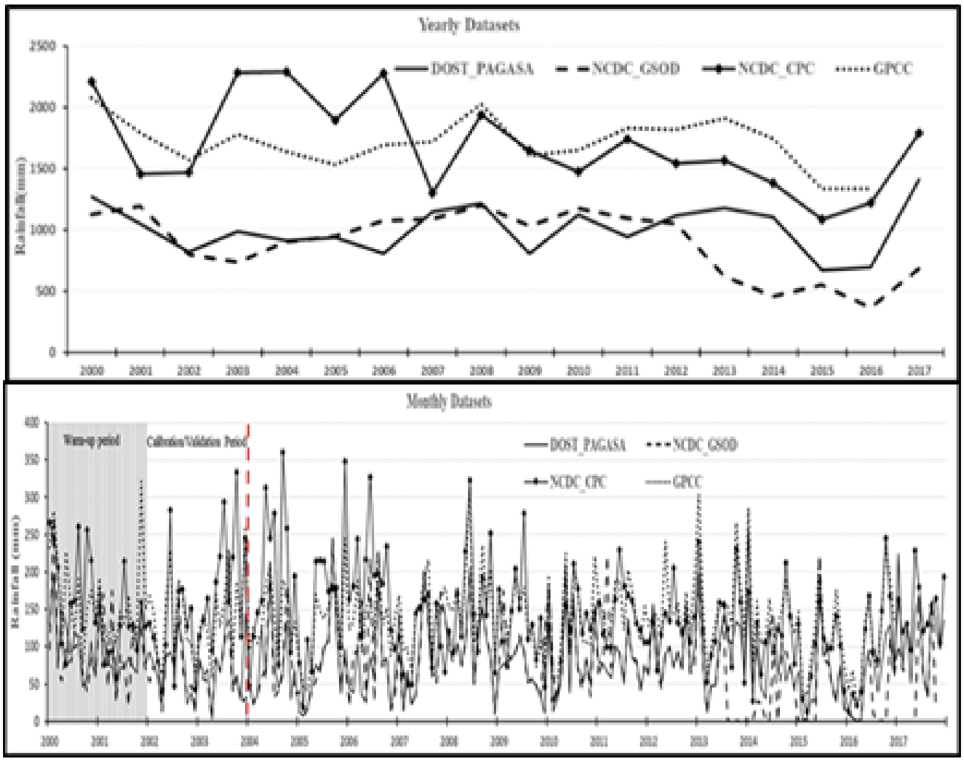

Figure 4: Total Yearly and Monthly Precipitation datasets from General Santos station and the nearest grid for GPCC and NCDC-CPC dataset.

2.2. Study Objectives

1) To simulate the watershed and validate the actual river discharges of the selected sub basins.

2) To improve the electricity in Mindanao.

    - Calculated/Estimated theoretical Potential hydropower
    - Distinguish the power capacity from pico, micro and large-scale hydropower.

3. Data Set and Methodology

3.1 Data Set

The data used in this research was obtained and downloaded from different government agencies and global climate data sets. The summary of the dataset is presented in the table below.

3.1.1 Rainfall and weather datasets

Since the SWAT modeling requires weather data as physical[9] based therefore the rainfall datasets were carefully examined and compared the gridded[2][3] and observed dataset of DOST-PAGASA stations in Mindanao. Subsequently, the correlation of rainfall datasets is followed; 0.78 for GPCC, 0.75 for NCDC-GSOD and 0.43 for NCDC-CPC. These values were computed based on monthly datasets as shown in figure 4. In addition, temperature, wind speed, humidity and solar radiation were also collected from the DOST-PAGASA station.

Data	Location/Type	Year/Duration	Description	Source	Format
Digital Elevation Model	Mindanao Island	2018	Raster derived from a RADARSAT Synthetic Aperture Radar (SAR), 10m resolution	Department of Science and Technology and University of the Philippines- Project. https://lipad.dream.upd.edu.ph/	GeoTIFF
Administrative Map	Mindanao Island	2015	Regional, Provincial, Municipal and barangay boundaries	Global Administrative Areas https://gadm.org/index.html Philippine GIS organization http://philgis.org/	Shapefile
Land use and land Cover	Mindanao Island	2010 - 2015	Land Sat 8 of 2010, 30m resolution, ground validation in year	National Mapping and Resources Information Authority, http://www.namria.gov.ph/	Shapefile
Soil Map	Mindanao Island	2007	Soil type and classification	Bureau of Soils and Water Management http://www.bswm.da.gov.ph/ Philippine GIS organization http://philgis.org/	Shapefile
Rainfall Records	DOST-PAGASA (General Santos)	1995 - 2017	Daily observed rainfall of Mindanao metrological stations	Philippine Atmospheric, Geophysical and Astronomical Services Administration, www.pagasa.dost.gov.ph/	Spreadsheet file
	NCDC-GSOD (General Santos)	1990 - 2017	Global Summary of the Day of daily observed rainfall	National Center for Environment Information https://www.ncdc.noaa.gov/data-access/quick-links#gsod	Text file
	NCDC -CPC (Gridded dataset)	1979 - 2017	Global daily precipitation with a spatial grid of 0.5^0 lat & 0.5^0 lon.	National Climatic Data Center ftp://ftp.cdc.noaa.gov/Datasets/cpc_global_precip/	NetCDF
	GPCC (Gridded dataset)	1982 - 2016	Global daily precipitation with a spatial grid of 1.0^0 lat & 1.0^0 lon.	Global Precipitation Climatology Center ftp://ftp.dwd.de/pub/data/gpcc/html/fulldata-daily_v2018_doi_download.html	NetCDF
Weather Records	Mindanao Station a) Temperature b) Wind Speed c) Humidity d) Solar Radiation	1995 - 2017 2016 - 2017	Observed daily datasets	Philippine Atmospheric, Geophysical and Astronomical Services Administration, www.pagasa.dost.gov.ph/	Spreadsheet file
Population	Mindanao Island	2010 – 2015	Census for Population	Philippine Statistic Authority	Spreadsheet file
Energy and Development Plan	Mindanao Island	2010 - 2017	Socio-Economic Conditions, Plans and Report.	Department of Energy, https://www.energy.gov/ Mindanao Development Authority, http://minda.gov.ph/ Bangsamoro Development Agency, https://bangsamorodevelopment.org/	Reports, Printed plans

3.1.2. Digital Elevation Model

The Digital Elevation Model was processed by the University of the Philippines for Applied Geodesy and Photogrammetry (UP– TCAGP), it was derived from Synthetic Aperture Radar (SAR) image with 10m resolution, and obtained from MacDonald, Dettwiler and Associates Ltd. (MDA), British Columbia, Canada through the

DOST-GIA funded Disaster Risk and Exposure Assessment for Mitigation (DREAM) Program. Moreover, DEM and Other geospatial datasets were projected with the Universal Transverse Mercator (UTM) Zone 51 projection and World Geodetic System (WGS) 1984 as the horizontal datum.

3.2. Methodology

The flowchart shows the modeling procedures and steps, it also illustrates the required software in every step, by then you can able to generate the outputs for algorithm processes and computations.

Figure 7: Model Flowchart

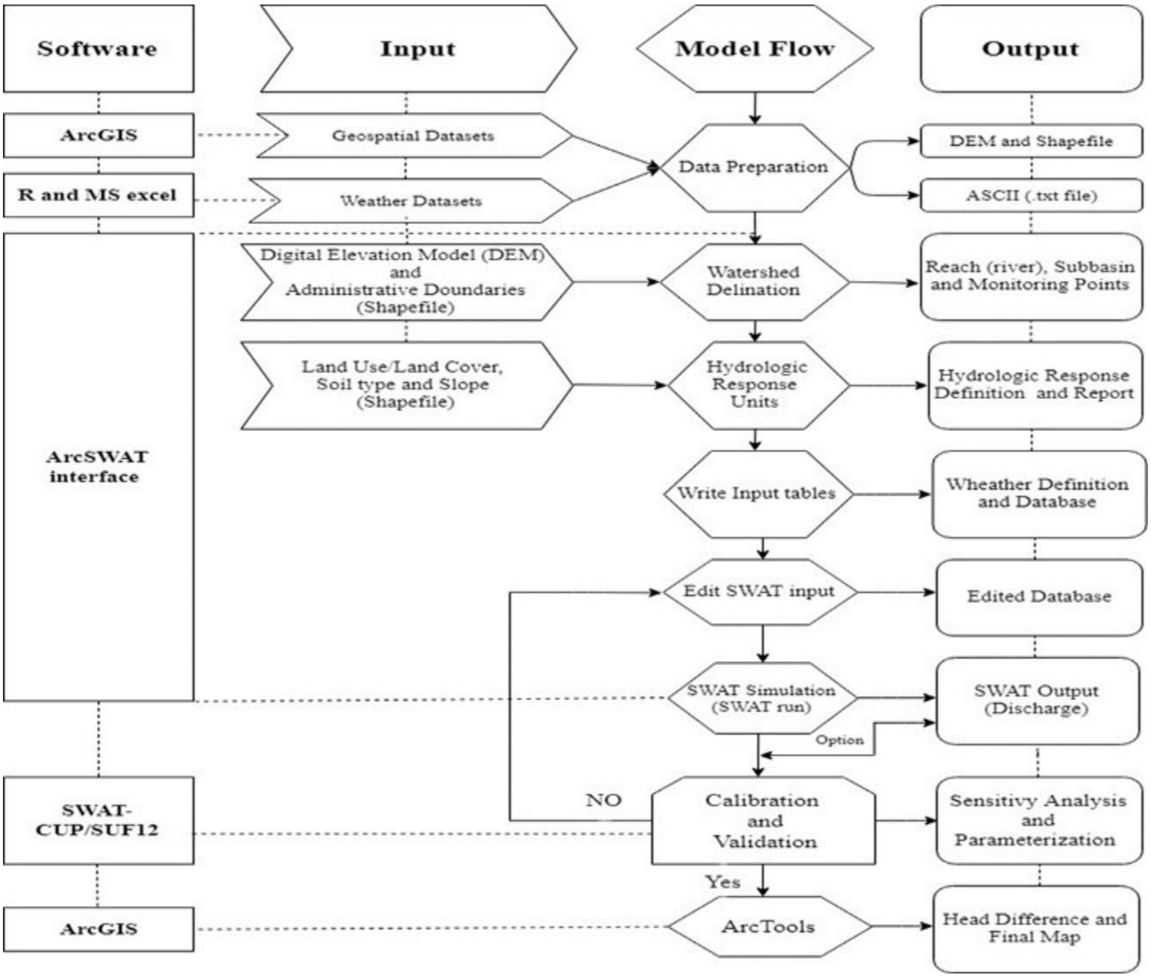

This basic procedure for modeling is clearly explained in the ArcSWAT manual and documentation[10][11]. Moreover, the SWAT modeling can be possibly done thru the open source GIS users, QGIS has a similar function to ArcSWAT [12]. Thus, QSWAT modeling is useful also for similar research methods. Basically, SWAT modeling is useful for long-term, and continuous simulation watershed model and designed to predict the impact of water management [9][13]. Also, it was developed to simulate the water cycle, and corresponding fluxes of energy to assess the impact of management practices [11][14]. Furthermore, "SWAT model has proven to be an effective tool for assessing water resource and nonpoint-source pollution problems for a wide range of scales and environmental conditions across the globe" [15]. It has the capability to evaluate sensitive parameters of streamflow [16] and determine the sensitivity of the parameters through SWAT-CUP[17][18].

3.3. Discharged and Power Calculation

3.3.1. Discharged

There are several methods to compute the theoretical discharges of river run-off. However, SWAT simulation employs the water balance for the hydrologic cycle by the given equation 1[9][11]. Discharge calculation is very important to compare the results between simulated and observed river discharged. Thus, these discharge formulas[11] to calculate the theoretical river discharge is given by equation 2 and 3. Basically, the rational modified[19] formula is from the rational and manning[20] formula that considered in the modeling[11].

Water Balance Equation: $SW_t = SW_0 + \sum_{t=1}^{t} (R_{day} - Q_{surf} - E_a - W_{seep} - Q_{gw})$ .... (1)

Modified Rational Formula: $Q_{peak} = \frac{\alpha_{tc} \cdot Q_{surf} \cdot A}{3.6 \cdot t_{conc}}$ .... (2)

SCS curve number equation: $Q_{surf} = \frac{(R_{day} - I_a)^2}{(R_{day} - I_a + S)}$ .... (3)

Manning formula: $V = \frac{1.486}{n} R^{2/3} \cdot slp^{1/3}$ .... (4)

Where SW_t is the final soil water content (mm H_2O), SW_0 is the initial soil water content (mm H_2O), Rday is the amount of precipitation on day (mm H_2O), Q_{surf} is the amount of surface runoff on day (mm H_2O), E_a is the amount of evapotranspiration on (mm H_2O), Wseep is the amount of water entering the vadose zone from the soil profile on day (mm H_2O), Q_{gw} is the amount of return flow on a day (mm H_2O), I_a is the initial abstractions which includes surface storage and S is the retention parameters, Q_{peak} is the Peak runoff rate (m^3/s), C is the runoff coefficient, A is the sub basin area (km^2), i is the rainfall intensity (mm/hr), 3.6 is a unit conversion factor, V is channel velocity (m/s), q_{ch} is the average channel flow rate (m^3/s), slp_{ch} is the channel slope, n is Manning's roughness coefficient for channel, α_{tc} is the fraction of daily rainfall that occurs during the time of concentration, t_{conc} is the time of concentration for the sub basin (hr), SCS is acronyms for Soil Conservation Service.

3.3.2. Power Calculation

Fundamentally, the power generated will be calculated by the given formula $\mathbf{P = \rho \times g \times Q \times h \times \eta}$; where P is the theoretical power in watts, ρ is the density of water (1000kg/m3), g is acceleration due to gravity (9.81 m/s2), Q is the volumetric flow rate in cubic meters per second, h is the head in meters, and η is the generator efficiency. The theoretical hydropower potential for each river segments is computed using the above formula of Power, the head difference of river is extract from the DEM using the reach output from the delineated watershed of the basins then it will be further generate through the algorithm in ArcGIS to specify the qualified head difference for power generation [21][22].

4. Results

The initial modeling results of Buayan Basin was obtained from the subbasin 12 in figure 5, and the discharged graph is presented in figure 6. The discharged shown in figure 6 illustrates that the gridded datasets of the rainfall produced better results compare to the datasets from the DOST-PAGASA. The correlation coefficient of simulated discharges from the observed is 0.72 NCDC-CPC, 0.60 GPCC, 0.35 DOST-PAGASA, and 0.15 for NCDC-GSOD. These results were not been calibrated yet due to the time constraint. However, it will be calibrated using SWAT-CUP in soonest possible time. Furthermore, these initial results of modeling draws already the different characteristics of the rainfall datasets, the DOST-PAGASA and NCDC- GSOD data sets always produced underestimated simulated discharges compared with the observed discharge while the gridded rainfall dataset sometimes gives an overestimated simulated discharged.

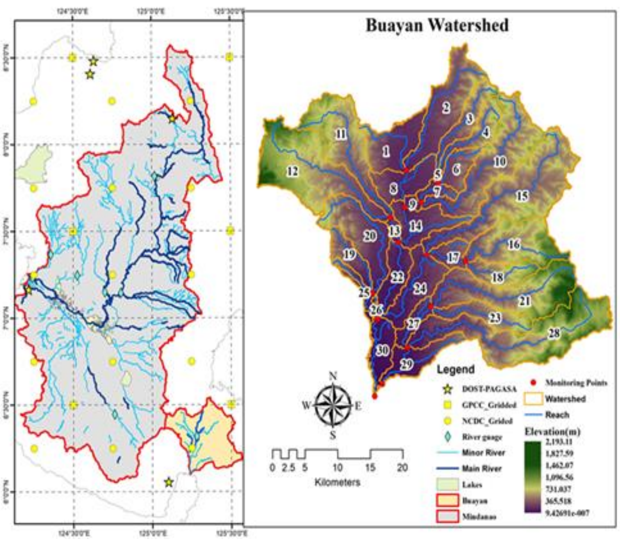

Figure 5: Detail maps of the Buayan basin; Delinated watershed from

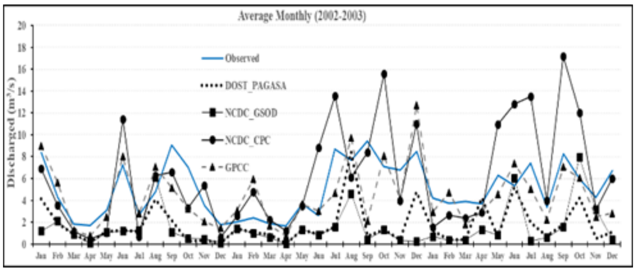

Figure 6: Initial results of modeling for Buayan Basin, the discharges were

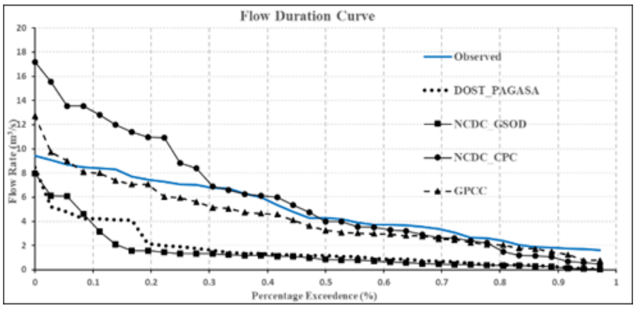

Figure 7: Flow-duration curve of the discharged against the percentage of

In addition, figure 7 represents the flow duration curves[22] for the discharges of the models. In this method the discharges used ranking from highest to lowest to get the percentage of exceedance. The graph shows that the probability of higher values of simulated discharges occurs around 30% for NCDC-CPC model and 20% for the rest of the models, while the observe discharged has smooth curve distribution of discharged probability. Hence, in this method the models have a calculated R^2 of 0.96 NCDC-CPC, 0.95 GPCC, 0.80 DOST-PAGASA, and 0.80 for NCDC-GSOD. In addition, this flow duration curve method is being used for assessing the turbine design and capacity[23].

5. Discussion and Limitation

This study is limited watershed modeling on the assessment of the hydropower potentials, its sites and theoretical power generation. It focusses only on the power generation assessment for hydro power as renewable energy. The study may not able to cover the detail land use and land cover proposals for the development of the region. This study will not consider the water potable resource due to the limitation of the data collected. However, in the future work the water potability, soil management practices and climate impact assessment might be considered in a given time [24][25].

6. Things to be done further

The following are the things to be done in order to achieve the objective of this study:

- Collection of further information on the causes of uncertainties
- Reading more related literature from high impact journal/papers.
- Improve the calibration analysis.

7. Conclusion

Assessment of theoretical potential hydropower potential can be done in several ways but in this study demonstrate the methods using SWAT modeling for the watershed delineation using several rainfall models to examine the required discharged of the rivers to set up hydropower potentials, and to evaluate the relations in terms of the output of the rainfall from gridded and observed datasets. Finally, to recommend on the sustainability for water and energy resource development in Mindanao.

References

[1] Philippine Statistic Authority, "The Philippines in figures: 2015," 2015.

[2] J. Cabrera and H. S. Lee, "Impacts of Climate Change on Flood-Prone Areas in Davao Oriental, Philippines," *Water 2018, Vol. 10, Page 893*, vol. 10, no. 7, p. 893, 2018.

[3] M. Chen *et al.*, "Assessing objective techniques for gauge-based analyses of global daily precipitation," *J. Geophys. Res. Atmos.*, vol. 113, no. 4, pp. 1–13, 2008.

[4] L. G. Ayson *et al.*, "Philippine Energy Plan 2012-2030," *Dep. Energy* , vol. 223, no. 410, 2010.

[5] DOE Report, "Power Supply and Demand Highlights Total Non-coincidental Peak Demand, Philippines in MW," 2017.

[6] National Grid Cooperation of the Philippines, "Transmission Development Plan 2014 -2015."

[7] Uniiversity of the Philippines, "Mindanao River: Dream Ground Survey Report," 2017.

[8] University of the Philippines, "Buayan-Malungon River Basin: DREAM Flood Forecasting and Flood hazard Mapping," 2015.

[9] J. G. Arnold, J. R. Kiniry, R. Srinivasan, J. R. Williams, E. B. Haney, and S. L. Neitsch, “Input/Outputs SWAT,” 2012.

[10] M. Winchell, R. Srinivasan, M. Di Luzio, and J. Arnold, “ARCSWAT INTERFACE FOR SWAT2012, USER’S GUIDE,” *Texas Agrilife Res. United States Dep. Agric. Agric. Reseach Serv.*, 2013.

[11] S. . Neitsch, J. . Arnold, J. . Kiniry, and J. . Williams, “SWAT Theoretical Documentation Version 2009,” *Texas Water Resour. Inst.*, pp. 1–647, 2011.

[12] Y. T. Dile, P. Daggupati, C. George, R. Srinivasan, and J. Arnold, “Introducing a new open source GIS user interface for the SWAT model,” *Environ. Model. Softw.*, vol. 85, pp. 129–138, 2016.

[13] M. Jha, “Hydrologic simulations of the Maquoketa river watershed Using SWAT,” no. June, 2009.

[14] H. Rathjens and N. Oppelt, “SWAT model calibration of a grid-based setup,” *Adv. Geosci.*, vol. 32, pp. 55–61, 2012.

[15] P. P. W. Gassman, M. M. R. Reyes, C. C. H. Green, and J. J. G. Arnold, “The Soil and Water Assessment Tool : historical development, applications, and future research directions,” *Trans. ASAE*, vol. 50, no. 4, pp. 1211–1250, 2007.

[16] L. A. Anaba, N. Banadda, N. Kiggundu, J. Wanyama, B. Engel, and D. Moriasi, “Application of SWAT to Assess the Effects of Land Use Change in the Murchison Bay Catchment in Uganda,” *Comput. Water, Energy, Environ. Eng.*, vol. 06, no. 01, pp. 24–40, 2017.

[17] K. C. Abbaspour, S. A. Vaghefi, and R. Srinivasan, “A guideline for successful calibration and uncertainty analysis for soil and water assessment: A review of papers from the 2016 international SWAT conference,” *Water (Switzerland)*, vol. 10, no. 1, 2017.

[18] K. C. Abbaspour, E. Rouholahnejad, S. Vaghefi, R. Srinivasan, H. Yang, and B. Kløve, “A continental-scale hydrology and water quality model for Europe: Calibration and uncertainty of a high-resolution large-scale SWAT model,” *J. Hydrol.*, vol. 524, pp. 733–752, 2015.

[19] R. Baxter, N. Hastings, A. Law, and E. J. . Glass, “Use of the Rational and Modified Rational Method for Hydraulic Design,” 2008.

[20] G. J. Arcement and V. R. Schneider, “Guide for Selecting Manning ’ s Roughness Coefficients for Natural Channels and Flood Plains United States Geological Survey Water-supply Paper 2339,” *United States Geol. Surv. Water-supply*, vol. 2339, no. 2339, p. 39, 1989.

[21] J. Jason, S. Garcia, A. Marie, L. De La Serna, M. A. Fesalbon, and J. R. Silapan, “Estimation of Hydropower Potential Energy Using Gis and Swat Hydrologic Model in Western Visayas,” pp. 1–8.

[22] J. L. Cuasay, G. C. Agno, D. A. Karl Mari Malonzo, R. A. May Fesalbon, L. V Camille Inocencio, and M. O. Rosario Concepcion Ang, “Evaluation of Climate Forecast System Reanalysis and local weather station data as input for run-of-river hydropower assessment in Agusan River Basin, Philippines,” 2014.

[23] S. C. P. B.C. Kusre , D.C. Baruah, P.K. Bordoloi, “Assessment of hydropower potential using GIS and hydrological modeling technique in Kopili River basin in Assam (India),” *Am. J. Manag. Care*, vol. 16, no. 6, pp. 459–466, 2010.

[24] H. Q. Bang, N. H. Quan, and V. Le Phu, “Impacts of Climate Change on Catchment Flows and Assessing Its Impacts on Hydropower in Vietnam ’ s Central Highland Region,” *Glob. Perspect. Geogr.*, vol. 1, no. 1, pp. 1–8, 2013.

[25] G. Cuceloglu, K. C. Abbaspour, and I. Ozturk, “Assessing the water-resources potential of Istanbul by using a soil and water assessment tool (SWAT) hydrological model,” *Water (Switzerland)*, vol. 9, no. 10, 2017.

[CHESS Lab semester summary seminar handout]

Optimized evacuation plan and decision support system development with Agent-Based Modeling (ABM) for Tsunami in Banten, Indonesia

Ricard Diago Sambuaga[1]

[1]Chess Lab., Department of Development Technology, Graduate School for International Development and Cooperation (IDEC), Hiroshima University

Abstract (Summary of Research Proposal)

On December 22, 2018, a tsunami caused by the eruption of volcanic mountain and partial collapse of the Mt. Anak Krakatau volcano occurred in the Sunda Strait, Indonesia. The tsunami that occurred in the Sunda Strait resulted in 430 casualties (January 7th, 2019). In this research, author use ArcGIS to create Banten map and netlogo for agent-based modeling (ABM). Data collection that needed in this research are DEM (Digital Elevation Model) and Infromation data (road network, hospital, coastline, etc.). and surveys. In this research, author proposed evacuation road and model-up in netlogo and compare evacuation time and casualty estimation with past event.

Keyword: *Tsunami, Evacuation, ArcGIS, Netlogo.*

1. Introduction

Indonesia is an archipelago country that has a high potential for natural hazards. This high potential is due to the location of Indonesia which is in the area of "ring of fire" and located between three large plates (India-Australia plate, Pacific plate, and Eurasian plate). This caused Indonesia to become an area that often experiences of volcanic eruptions and earthquakes. Because of this condition, Indonesia has a high potential of tsunami as well. Figure 1 describes the ring of fire and Indonesia location between three large plates.

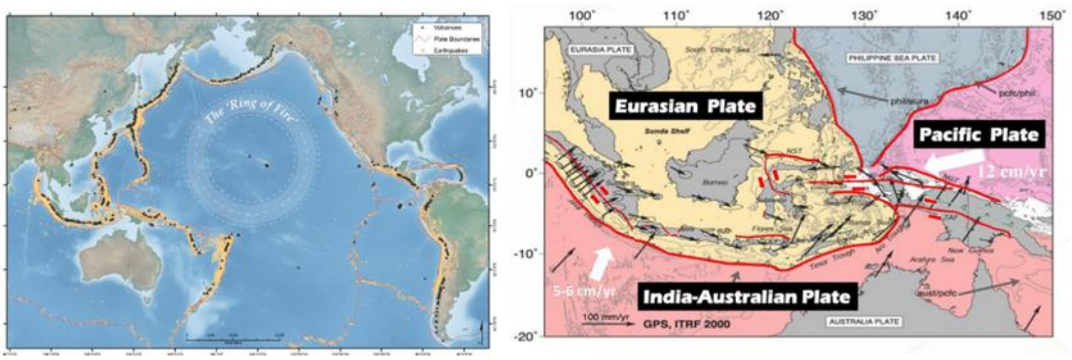

Figure 1 (a) Ring of fire in Indonesia and (b) Geographical Zone of Indonesia

[CHESS Lab semester summary seminar handout]

Table 1 Indonesia Tsunami historical data

Year	Number of events	Fatalities (person)		Houses (unit)				Damaged (unit)		
		Wounds or Injury	Suffer and Evacuate	Huge Damaged	Moderately Damaged	Lightly Damaged	Submerged	Health Facilities	Worship Facilities	Educational Facilities
2014	2	0	0	0	0	0	0	0	0	0
2012	3	9	0	0	0	5	0	0	0	0
2011	1	0	67	17	0	17	0	2	1	0
2010	1	498	15,353	517	0	204	0	5	7	6
2006	3	520	6,727	1,777	0	585	0	4	22	8
2004	2	4,662	522,462	179,312	0	0	0	240	2,742	1,226
1998	6	0	381	0	0	0	0	0	0	0
1994	1	0	0	0	0	0	0	0	0	0
1992	1	0	0	0	0	0	0	0	0	113
1991	1	0	0	0	0	0	0	0	0	0
1979	1	0	171	0	0	0	0	0	0	0
1977	4	273	0	0	0	0	0	0	0	1
1973	1	0	0	0	0	0	0	0	0	0
1907	1	0	0	0	0	0	0	0	0	0
1861	1	0	0	0	0	0	0	0	0	0

Based on the conditions mentioned above, the following tables present statistical data of tsunamis affecting Indonesia. Table 1 shows that the statistical data of historical tsunami events in Indonesia. From the data above, we can find that the high incidence, number of casualties, and losses due to tsunami in Indonesia need to special attention in the future, so these numbers can be reduced. Natural hazard in Indonesia cannot be avoided, but we can reduce the potential for high rates of casualties and losses.

On December 22, 2018, a tsunami caused by the eruption of volcanic mountain and partial collapse of the Mt. Anak Krakatau volcano occurred in the Sunda Strait, Indonesia. Figure 2 describes the location of Anak Krakatau in Sunda Strait. The Sunda Strait is a strait located in Indonesia that connects Java and Sumatra islands (Banten Province, Java – Lampung Province, Sumatra). It connects the Java Sea to the Indian Ocean. Anak Krakatau (Child of Krakatoa) is a volcanic mountain located on the Sunda Strait. Anak Krakatau emerged from below of sea surface (1927) which occurred because of a large explosion of Mount Krakatau (1883) impact which was one of the largest volcanic explosions in the world. Volcanic activity from Anak Krakatau is still active today. Because of the eruption of Anak Krakatau, the height Anak Krakatau is increased by 4-6 m/year. The tsunami that occurred in the Sunda Strait resulted in 430 casualties (January 7th, 2019) [1].

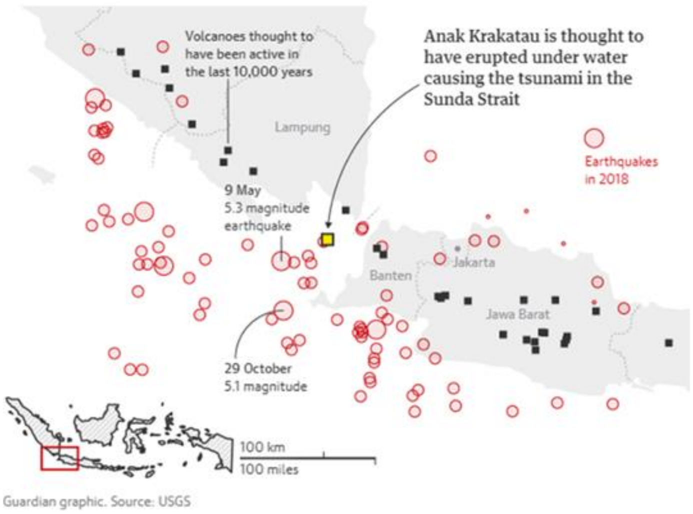

Figure 2 Anak Krakatau Location in Sunda Strait, Indonesia

To re-evaluate the tsunami event during the master course, it needs to collect some data. The data collections include surveys, statistical data from the event, and infrastructure data. This data will be processed using Geographic Information System tool (Arc-GIS). The output from processing the data is a map. The output of the Arc-GIS then will be used as input to the Agent-Based Modeling (ABM) simulation as a simulation environment.

This research will be started on inputting data of an existing environmental condition of a past event (infrastructure), such as population data, evacuation route design, shelter location and capacity, road network, and hazard map. The evacuation time of the evacuation route will be simulated by using ABM simulation. The result of ABM (existing condition) will be evaluated and the author will propose a new infrastructure condition (shelter location, evacuation route, etc.). ABM can model up to individual behavioral levels as well as adaptation processes that allow for the change of individual nature. It also helps in modeling the system, so the modeling will be very similar to reality. ABM can also simulate the evacuation phenomenon in detail and provide information from existing systems such as casualties that may exist during the evacuation process.

The author will use the NET-logo software in modeling the evacuation of an accident in this research. This software is well known as a pedestrian dynamic simulation. There is several software based on this theory such as VEGAS, LEGION packages, maritime EXODUS which developed by Greenwich University, Simulex and AnyLogic [2]. In this theory, each individual could be modeled to have own and continuous coordinate representing its location. It is also can be used as well for considering the physiological condition of the concerned person. The advantage of Net-logo is easier compared to another ABM software [3].

There is a tool in NET-logo software called BehaviorSearch. Behavior Search can be used to provide a low threshold way of looking for a combination of model parameters that will result in a specified target behavior [4]. BehaviorSearch could help an author to know which agent (resident) that took the longest time to evacuate and which agent that become a casualty in the event. NET-logo can model the evacuation process and calculate the time of the simulation. The result of the evacuation process will be evaluated and compared with the proposed infrastructure condition. The result of this comparison is to determine which evacuation plan is the most optimum in case of a tsunami.

2. Objectives

The expected results of this study are followings.

1) Provide optimum evacuation route.
2) To know the time required by residents to reach the Assembly Point based on ABM modeling results.
3) To know the casualty estimation of residents based on ABM.
4) To know the effect of tsunami influences decision-making based on many different scenarios.

3. Data and methodology

3.1 Data

Collecting data are needed to complete the research. Collecting data is a critical point of this research because all data will support writing the research. Collecting data needed in this research are divided into two groups. Detail data collection shown in Figure 3.

The first group is survey, Revealed Preference (RP) Survey and Stated Preference (SP) Survey [5]. RP is designed to collect data that describing actual travel or evacuee behavior. SP is a hypothetical behavior in the future, means a survey that describing what evacuee or residents should be when tsunami cases. RP is related to past tsunami event and SP is related to a future tsunami event.

The second group is related to Digital Elevation Model (DEM) data. These data are needed to create an actual infrastructure condition of an event. Population data, evacuation route design, shelter location and capacity, road network, and hazard map are needed as an input for ABM. These data are needed to evaluate the past actual infrastructure condition.

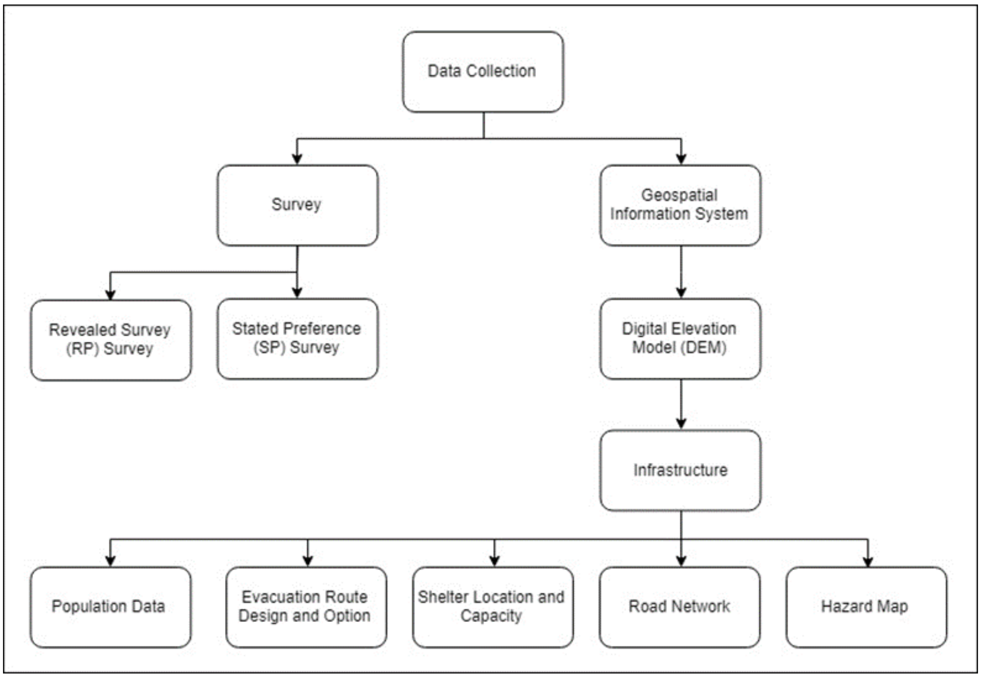

Figure 3 Detail data collection

3.2 Methodology

Detail methodology on this research is described in Figure 4.

1) Agent-Based Modeling

Infrastructure data that already collected are needed as an input for ABM simulation. These data will become a background for ABM. Background means it will become an environment condition for the simulation. Environment condition for this simulation is not only provided by DEM data but also provided by Tsunami modeling as well.

ABM will be assisted with NetLogo software. In this simulation, an analysis is using several assumptions and scenarios. NetLogo can provide to evaluate the evacuation process such as time calculation and casualty estimation based on tsunami modeling input. The results of this analysis are how the above environmental factors influence the behaviors of residents during the evacuation process, how to determine resident distributions, how much time it takes for evacuation process also casualties estimation due to tsunami event.

Agent behavior assumption for this modeling is divided into several groups. Those groups are vision ability, congestion and bottleneck condition, movement speed, grid area, and collision avoidance. Vision ability for each agent could de different due to day or night. Movement speed of this assumption is divided into two groups, those are ages and vehicles [6]. All assumption will affect the evacuation process for each agent.

In this simulation, author will be using three different scenarios. Those scenarios are start time approachment, four different types of evacuation trigger [7], and route option. Evacuation trigger is divided into four types, those are: ground shaking, tsunami warning, see other evacuating, and after seeing the tsunami. The output of this simulation is evacuation process time and the number of total casualties. Detail ABM is shown in Figure 5

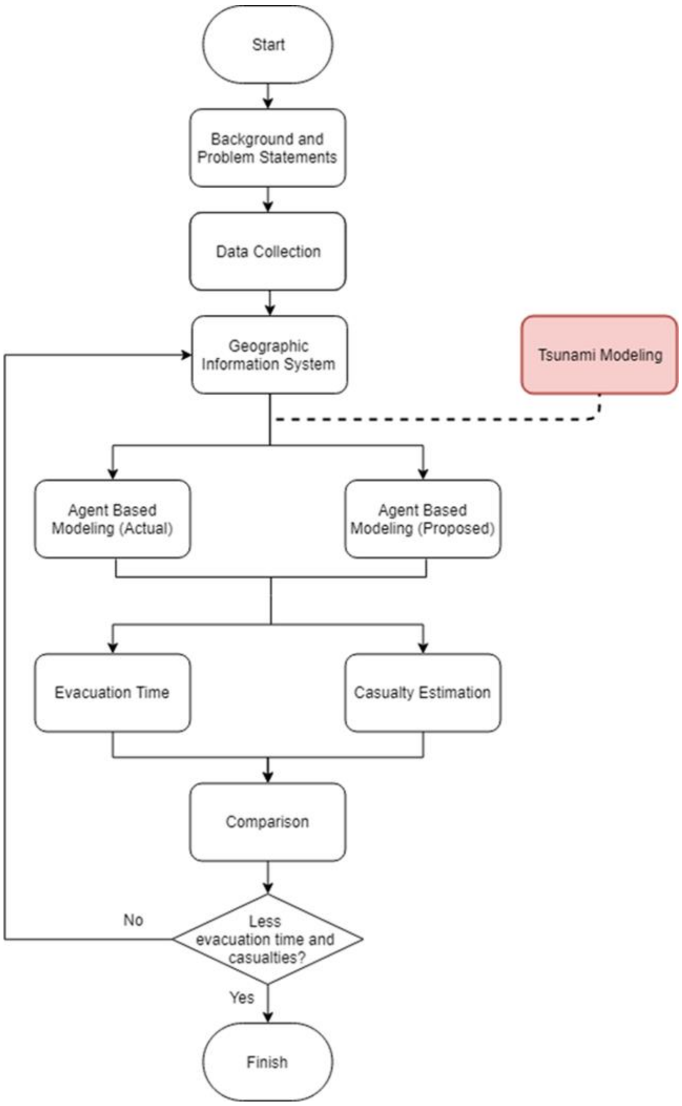

Figure 4 Methodology and flowchart of the proposed research

2) Time calculation of evacuation process and time comparison

In this phase, total evacuation time and total casualties is output from the ABM. The comparison is needed in this phase because the author wants to reduce the evacuation process time and number of casualties. The comparison in this section is comparing the actual infrastructure condition with the proposed infrastructure condition (proposed evacuation route map, shelter location, etc.). If the proposed infrastructure condition took a longer time and get a higher number of casualties, so the next step is re-arranged proposed infrastructure condition. If the proposed infrastructure condition took a lesser evacuation time and total casualties are lower, it will continue to the conclusion phase.

3) Conclusion

This phase is a summary of this research based on the data analysis and ABM modeling and what can be learned from this research. The final step is to make the conclusion based on the main findings and limitations of this study as well as to provide recommendations to existing problems.

Giving suggestions in this phase are being made to reduce the possibility of similar dangers. Mitigation suggestion is a solution to prevent recurrence of similar accidents. Conclusion and recommendation from this research are how to determine the most optimum evacuation route and how to reduce the time for evacuation process, and how to reduce a total number of casualties based on Agent-Based Modeling Simulation and comparison with proposed infrastructure condition.

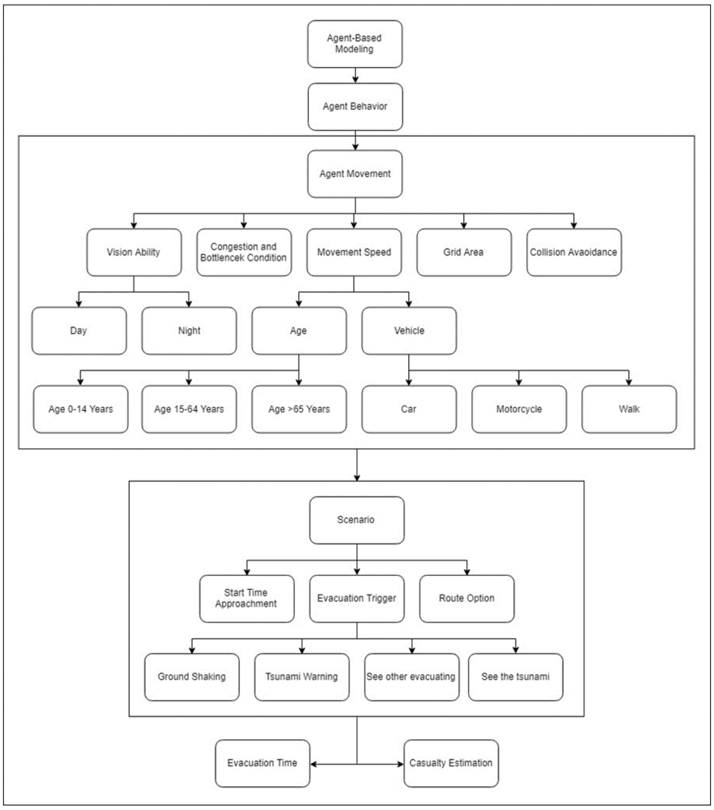

Figure 5 Detail Agent-Based Modeling (Framework)

4. Results

Results of this research are map of Banten, Indonesia and interface of netlogo model (environment data). Banten map in this research is processed by using ArcGIS software. Data are collected from government DEM data website with the resolution is 7 (seven) meter. The data that got from website is geodatabase (.gdb) format, after that data are processed using *mozaic* in arcgis to combine all data. After that, all information data also imported into this map. The result of Banten map on arcgis are describe in Figure 6 and Figure 7.

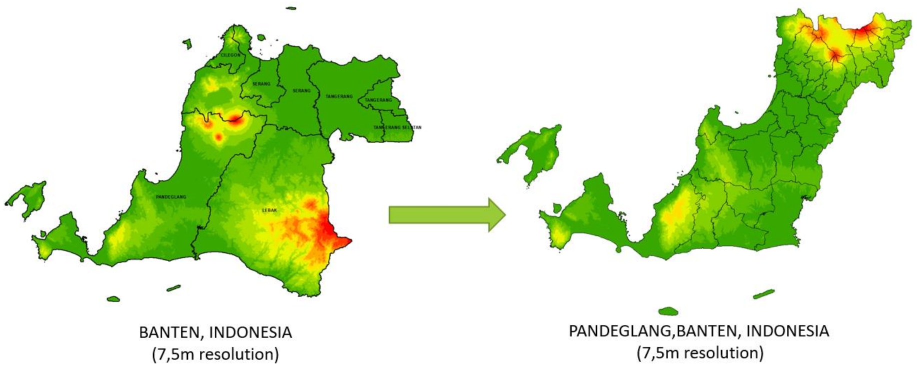

Figure 6 Pandeglang Map on ArcGIS Interface

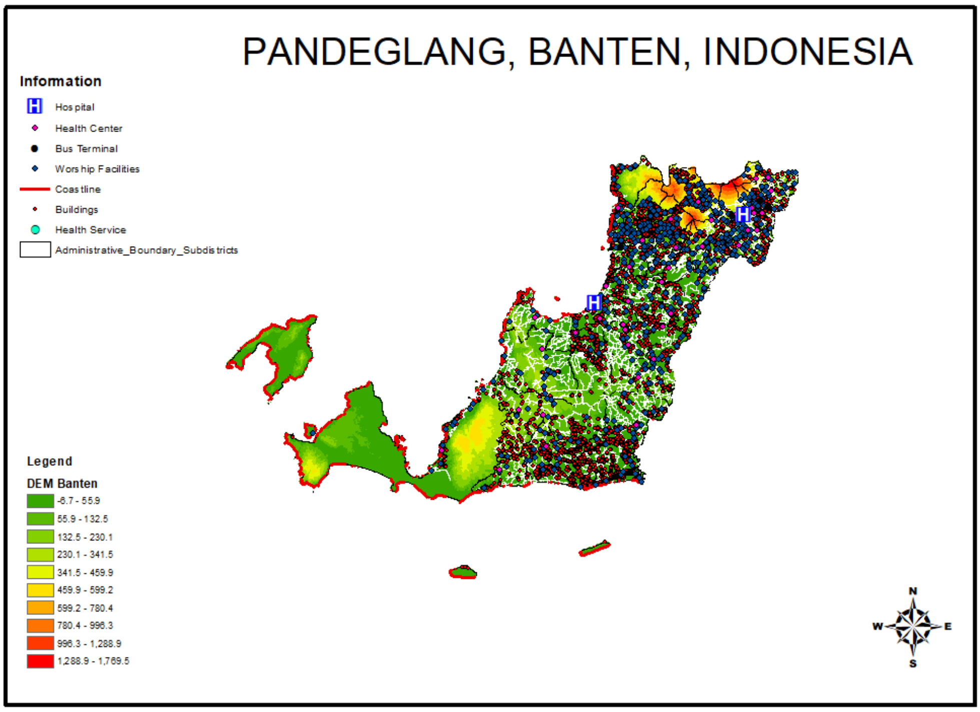

Figure 7 Pandeglang Map on ArcGIS Interface

Banten map is already done on ArcGIS interface, the next step is importing those map data on Netlogo. Import GIS data to Netlogo cannot be done directly because for format data should be adjusted first. Netlogo only can import data from GIS in (.prj), (.asc) or (.grd) format for raster (elevation) file and (.shp) format for vector dataset (Information data: road network, hospital, coastline, etc.). Figure 8 is described about step for importing data from arcgis to netlogo. Aggregation is needed to resize data to become smaller because netlogo cannot process with a big size data.

Figure 8 Import data from arcgis to netlogo

Importing (.shp) file to netlogo should be change the format also. (.shp) file from arcgis should be processed by using *featureclass*. Feature class is needed to convert my previous data which has x,y,z, and m information into (.shp) file with x and y information only. Converting data is needed because netlogo cannot process z and/or m information. The reason of this condition is my model on netlogo only 2D (Dimension), so z and/or m informations are not needed. Figure 9 and Figure 10 are describing an interface of raster data and information data on netlogo. There are several buttons on my netlogo interface. Those are *Setup, Display-Elevation, Recolor-patches, and Load. Setup* is main/default interface in my model, *Display-elevation* is displaying an import raster (elevation) data from arcgis to netlogo, *recolor-patches* is a recolor raster data from arcgis in pixel form, and *load* is displaying all information data from arcgis to netlogo.

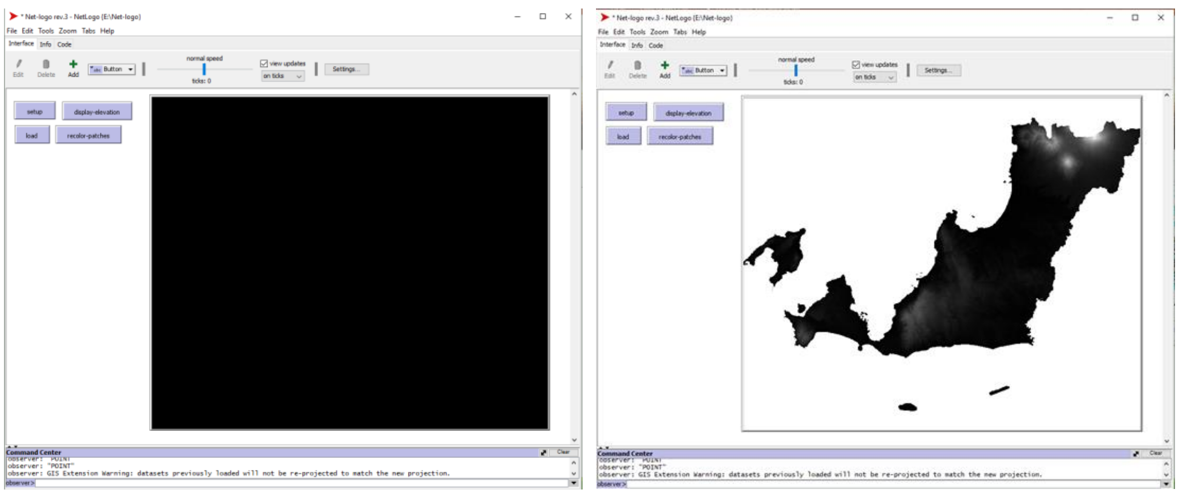

Figure 9 (a) *Load* and (b) *Display-Elevation*

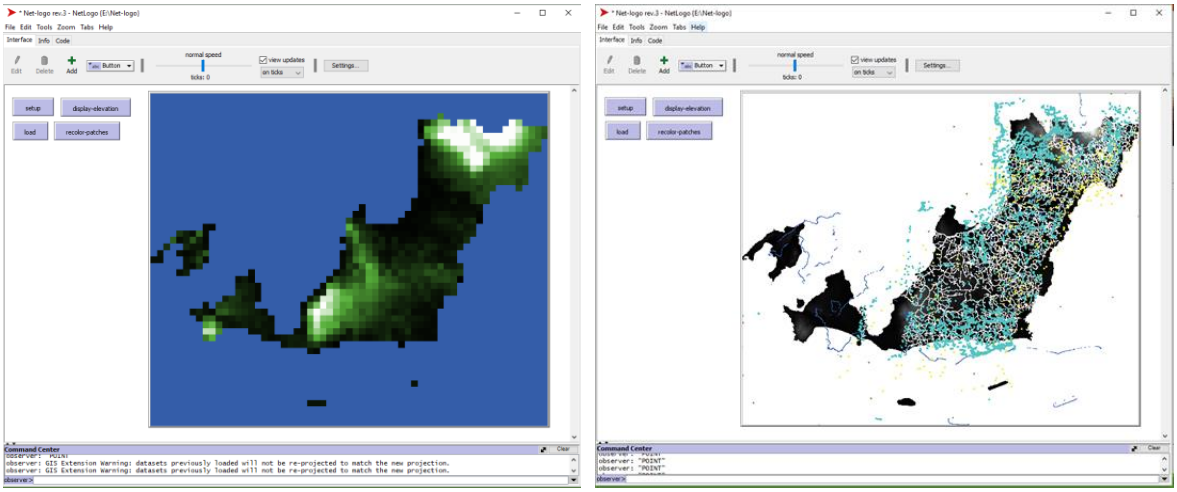

Figure 10 (a) *recolor-patches* and (b) *Load*

5. Discussion and Limitation

This semester, author face some problem in this research. These problems are:

1. Raster data color on netlogo still black and white. Author need to change raster color, so the elevation difference can be seen clearly.
2. The coordinate of all information data such as hospitals, road, coastline, etc. data has not fit with the raster data on netlogo interface.

6. Things to be done further

1. Improve the interface of arcgis "import data" on netlogo. (problem with the coordinate of each information data).
2. Create a simple modeling in netlogo based on environmental data. (Creating agent, combining with environmental condition).
3. Input an agent behavior on netlogo modeling.

References

[1] J. Amos, "Anak Krakatau volcano_ Satellites get clear view of collapse - BBC News." BBC Science Correspondent, United Kingdom, 2019.

[2] T. Pitana and S. Member, "Passengers Evacuation Simulation in a Cruise Ship due to Tsunami Attack as Port Safety Management Consideration," 日本船舶海洋工学会論文集, vol. 7, pp. 55–64, 2007.

[3] G. Kanjilal, B. Rajgire, V. Kumar, J. M. Tech, and S. Technology, "Netlogo simulation : effective for agent based modeling in artificial intelligence," *Int. J. Recent Innov. Trends Comput. Commun.*, vol. 1, no. 3, pp. 159–160, 2014.

[4] F. Stonedahl and U. Wilensky, "Finding Forms of Flocking: Evolutionary Search in ABM Parameter-Spaces BT - Multi-Agent-Based Simulation XI," 2011, pp. 61–75.

[5] E. MAS, A. SUPPASRI, F. IMAMURA, and S. KOSHIMURA, "Agent-based Simulation of the

2011 Great East Japan Earthquake/Tsunami Evacuation: An Integrated Model of Tsunami Inundation and Evacuation," *J. Nat. Disaster Sci.*, vol. 34, no. 1, pp. 41–57, 2012.

[6] E. Mas, "Geospatial Simulation of Tsunami Evacuation Using Gis Data and Agent Based Modeling," 2014.

[7] T. Takabatake, T. Shibayama, M. Esteban, and H. Ishii, *Advanced casualty estimation based on tsunami evacuation intended behavior: case study at Yuigahama Beach, Kamakura, Japan*. 2018.

[CHESS Lab semester summary seminar handout]

Mitigation techniques to reduce renewable energy curtailment

Alex Bunodiere

Hiroshima University

Abstract

Increasing renewable energy penetration is a relatively new phenomenon in Japan and while the penetration in Japan is still quite low, in some areas the penetration is very high such as Kyushu. In Kyushu the RE penetration is very high, accounting for up to 50% of the energy supply. This high penetration has led to the first ever RE curtailment in Japan occurring in Kyushu in October 2018. This curtailment is only going to get worse, as RE penetration continues to increase and nuclear energy increases in line with Japan 2030 energy goals and the population decline which will lead to lower demand, especially in rural areas. In order to prevent this curtailment and increase energy stability, several mitigation methods will need to be developed and implemented to help maintain the stability of the grid and financial prosperity of privately owned RE developers.

1. Introduction

The energy sector in Japan has changed dramatically post Fukushima disaster with a large increase in solar PV penetration due to a high feed-in tariff (FIT) that incentives private developers to build solar PV across the country and sell their electricity to the local power company. Some regions have seen higher development of solar PV due to low land cost, relative to the rest of Japan, namely Kyushu and Hokkaido as can be seen below with a ratio of peak demand to PV at a maximum of about 40%. This very high growth rate is good for the energy self-sufficiency of Japan which has been decreasing since the Fukushima disaster and the environment, however it presents some challenges to the utility company as they have to be able to match the electricity supply and demand and if a variable source of electricity such as solar is introduced without implementing any kind of demand management or large storage then there is a risk of RE curtailment as what happened in October 2018. The reestablishment of nuclear energy along with RE will add extra pressure on the utility company.

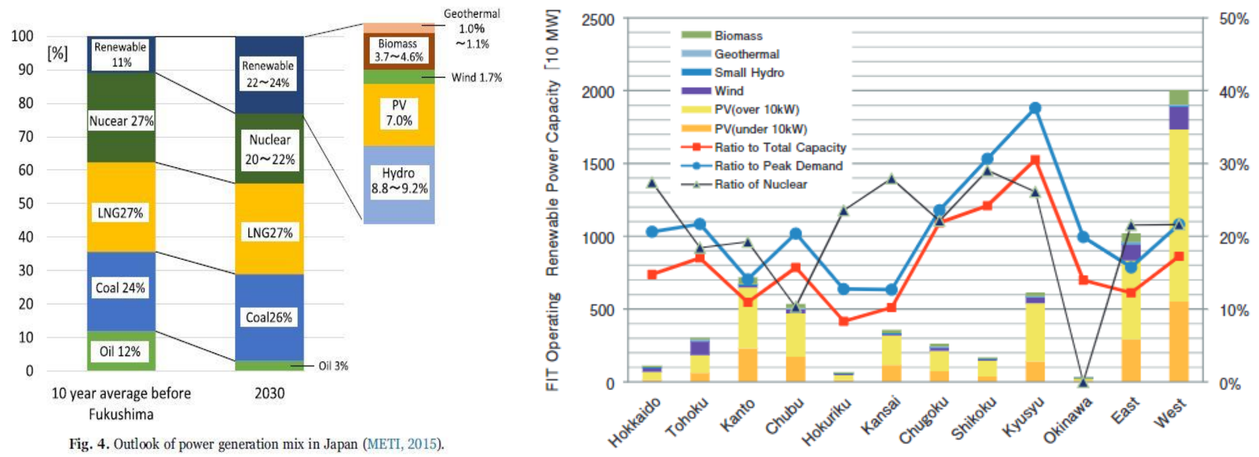

Figure 11: Outlook of power generation mix in Japan 2030 and installed capacity of RE vs total demand

RE Curtailment had never occurred before however there is a provision for it in the FIT agreement, it states that "grid operators can enforce curtailment against renewable electricity producers without compensation up to 30 days per facility per year to balance supply and demand and are obliged to compensate for curtailment over 30 days. Further, grid operators can refuse connection agreements when curtailment is anticipated to go over 30 days"(Kimura, 2017)

This means that utilities can curtail RE without compensation for up to 30 days a year, which is 12% of the year. This rule is quite unique as most other countries have rules to partially or fully compensate during curtailment. (Bird et al., 2016) The reason for this is for investor security, if a RE plant can lose up 12% of its revenue in a year, it may mean that that plant will not produce any profit in that year, and since the RE plants have no control on when or if the curtailment occurs, they are completely at the mercy of the utility. Since the first curtailment has occurred in Kyushu, 22786MWh of solar PV and 226MWh of wind has been curtailed (As of January 1st 2019) and while this is still quite small in terms of percentage compared to total PV and wind generated, see table below, this is a marked increase from 2017 where no curtailment occurred.

Table 2: Solar PV and wind energy generated and curtailed in Kyushu

	Generated	Curtailed	Percentage curtailment 2018	Percentage curtailment 2017
Solar PV	9765961MWh	22786	0.23%	0%
Wind	587447MWh	226	0.04%	0%

While this curtailment is still quite small, the problem is that the RE penetration is set to increase, while the demand is set to decrease, especially in areas with large rural populations like Kyushu. These two factors will lead to increased curtailment not only in Kyushu but Hokkaido and then the rest of Japan after that. Curtailment is also not the only issue, due to limited grid connectively between regions in Japan, if a disaster occurs or there is a surplus or deficient in electricity, there isn't enough capacity to transfer electricity to other regions. Kyushu and Hokkaido are particularly venerable to this due to their limited connection to only one other prefecture.

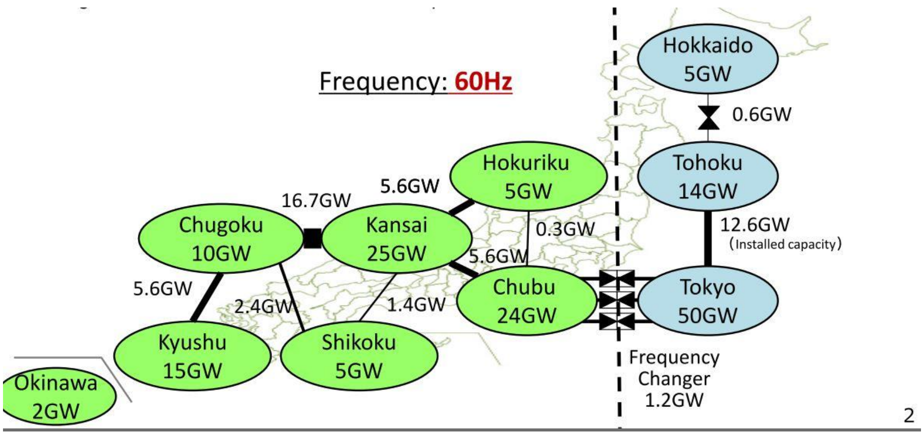

Figure 12: Intergrid connectivity and capacity 2016 (SHINKAWA, 2018)

2. Objectives

To predict future curtailment across Kyushu and possible the whole of Japan considering increased RE penetration and decreasing population, and then be able to show how several mitigation techniques could reduce this curtailment, including quantity and savings due to these mitigation techniques. Finally, to make recommendations for the implementation of these techniques and their cost to benefit ratio.

3. Data and methodology

3.1 Data

The main collected secondary data is supply and demand data for Kyushu electric for the years 2016 – 2018. This data contains the actual electricity demand and different type of electricity supplies to meet that demand at an hourly resolution. This data was sourced from the Kyushu electric website and freely open to download. (Kyushu Electric, 2019) Along with the supply and demand data, predicted and actual electricity supply from both wind and solar has also been collected from the same website. (Kyushu Electric, 2019) This data is also for the years 2016 – 2018 and is in 30-minute intervals. Below is the percentage distribution of predicted solar vs actual solar for 2017. The graphs show the same data, the graph on the right just sums all % difference of above 100%. A negative percentage means actual solar was higher than predicted (Under prediction) while a positive percentage means actual was lower than predicted(Over prediction). Count of + values is 4391, Count of – values is 4530 (Slightly higher number of underprediction) however magnitude is a different average of + values is 100.81% while average of – values is -21.19% (Significantly Higher quantity overprediction). The result is that there is a significant difference between the predicted solar and actual solar, which may lead to problems with managing supply. The distribution per season is also shown with higher over predictions in autumn and higher under predictions in spring.

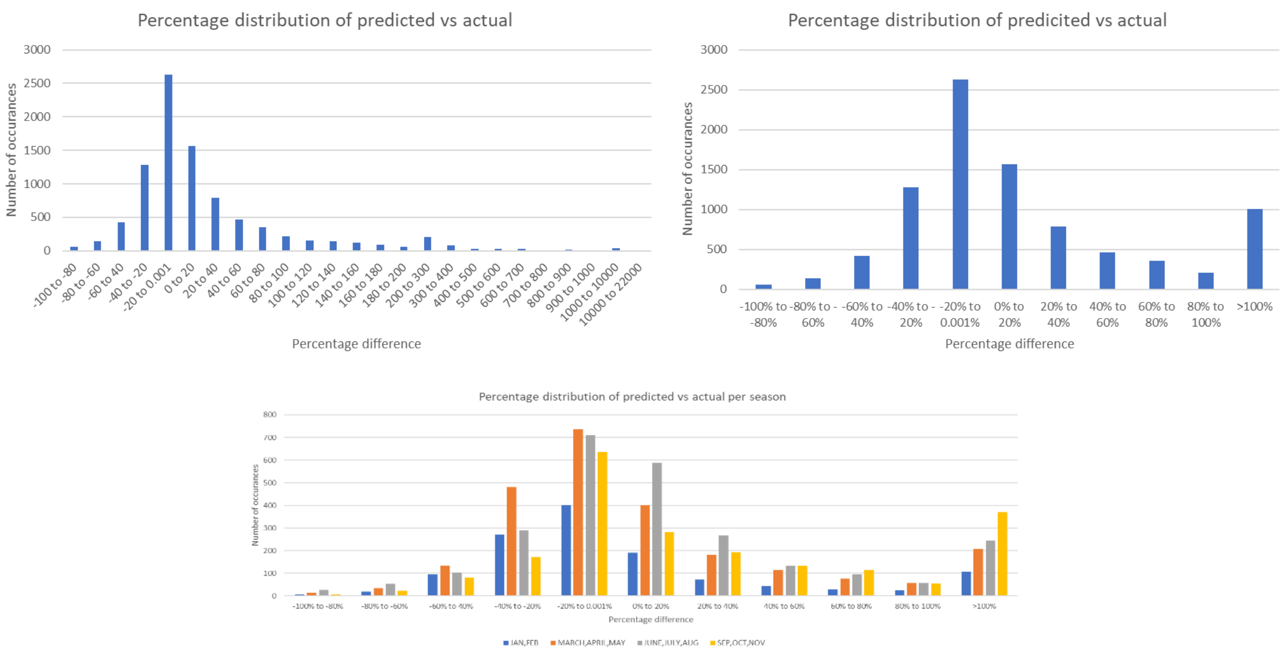

Figure 13: Percentage distribution of predicted vs actual solar 2017 and distribution according to season 2017

Below is a brief explanation of each data type collected and some observations for the year 2018. It's important to note that all of these graphs have actual electricity produced on the y-axis in MWh.

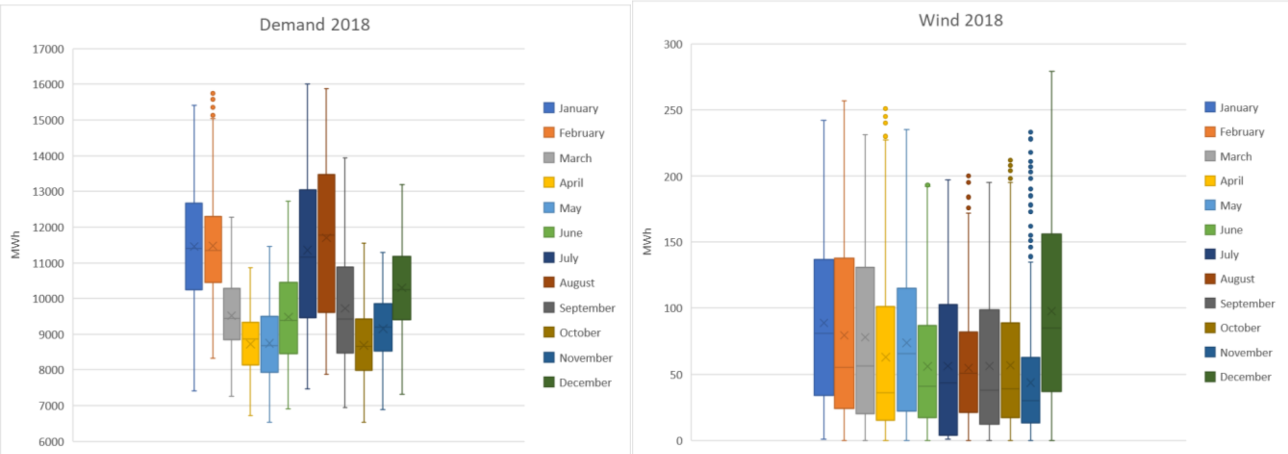

Figure 14: Electricity demand and wind energy supply for Kyushu 2018

The demand for Kyushu for 2018 shows the monthly trend for electricity demand. Electricity demand is highest in winter and summer months, most likely due to high air conditioner use to heat and cool areas respectively. The demand then drops in the spring and autumn months, again most likely due to the more comfortable temperatures requiring less aircon use. Fukuoka is in the south of Japan so it experiences more temperate temperatures compared to that of Hokkaido in the North. It is also interesting to note the difference between the max and min values throughout the year. These occur in the summer and winter months mostly and can be difficult for the utility to manage. The wind graph is more consistent with the highest generation in the winter months. It's worth noting however that the wind penetration in Kyushu is quite low, so the wind energy's effect is quite minimal.

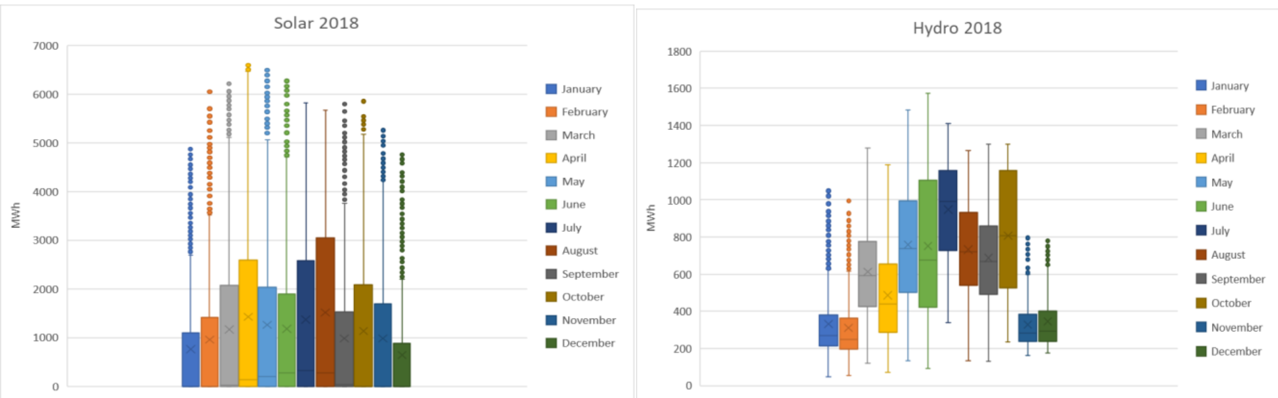

Figure 15: Solar energy and hydro energy for Kyushu 2018

The solar energy is quite interesting, as expected the peak generation occurs during summer months, but the difference between summer and winter months may not be as big as expected. This may be due to the temperate weather in Kyushu as well as the rains that occur in the summer months. It is also interesting to note that the max PV generation occurred in April, during spring and during the lowest demand time. The hydro generation is follows expectations with the lowest generation in the late autumn and winter months and increasing production during the summer time due to the rain season occurring during summer months.

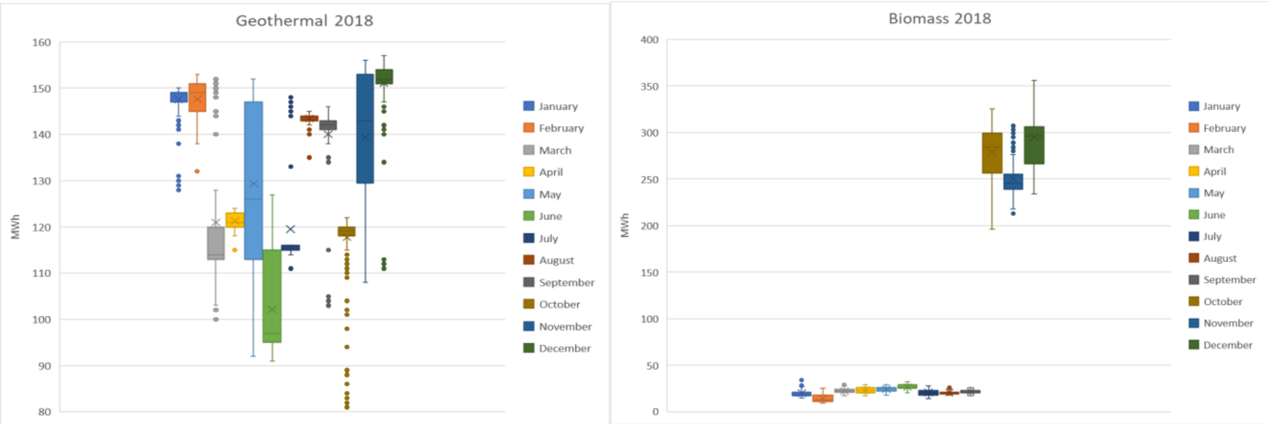

Figure 16:Geothermal and Biomass energy for Kyushu 2018

The geothermal energy generation is quite spread out across the different months of the year, for reasons that are unknown as of now, whereas the biomass was very consistent, except for October, November and December where the output increased 10 fold. This appears to be a data anomaly and is slated as one of the questions for Kyushu electric.

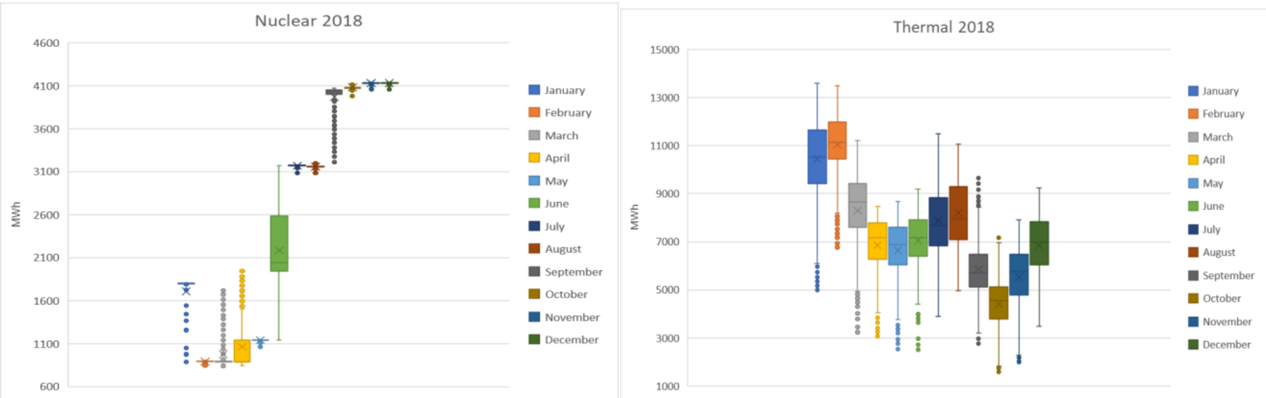

Figure 17: Nuclear and thermal energy for Kyushu 2018

The nuclear energy is quite consistent as would be expected, and it is clear to see the sudden increases in generation which are due to Kyushu reactivating several nuclear power plants. As these power plants continue to get reactivated as part of the 2030 energy plan, together with the increased RE will put added pressure on the utility, and may lead to more curtailment. The thermal energy graph shows large variations between max and min and wide range of mean values, this is because thermal energy together with pumped storage are the two main control measures that change according to RE energy supply, due to its ramp up/ ramp down speed. The thermal graph is almost the exact same shape as the supply graph, which makes sense since thermal energy is still the biggest supply of energy in Kyushu and Japan as a whole.

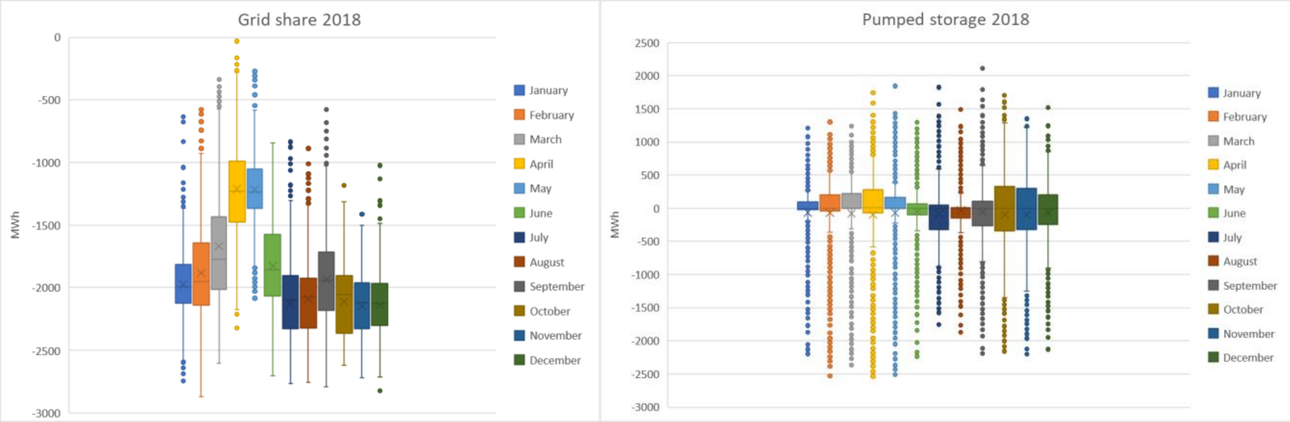

Figure 18: Grid share(negative values) and pumped storage for Kyushu 2018

Next is the grid share graph which shows the grid share to Chugoku region. The relationship of how this is controlled is unknown as of yet, although it is one of the proposed questions for Kyushu electric. From observation its clear that there is an decrease during the spring months which correlates with the low demand at the same time with the highest average values in the winter, autumn and summer months. This still requires some investigation. Lastly the pumped storage varies greatly across the year, due to its use in controlling supply to meet demand along with thermal power. It is used to storage energy when there is too much energy and release that energy later when required. One strange note about the pumped storage is that its clear to see that there is more negative values than positive and in fact the energy efficiency of this pumped storage is only 53% which is well below the international standard of 80%.(Trevor M. Letcher, 2016).

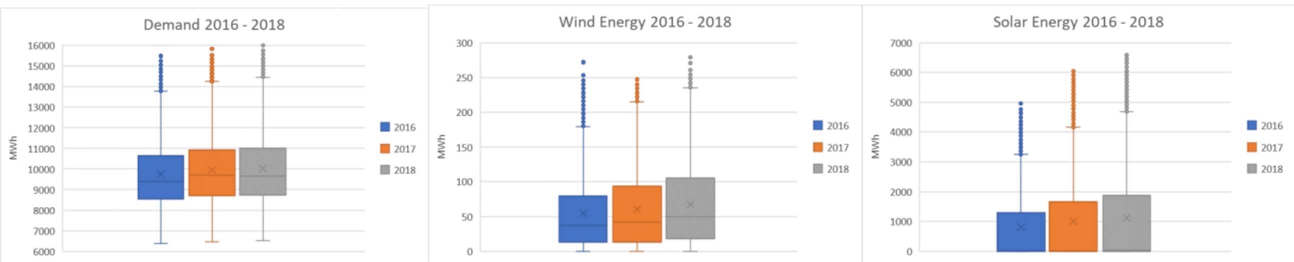

Figure 19: Electricity demand, wind energy and solar energy for Kyushu 2016 - 2018'

Comparing demand, wind energy and solar energy production the main interesting point is the slight increase in demand, with similar max and min points, the increase in wind energy with similar max points to 2016 and finally solar with a significant increase between 2016 – 2018.

As part of the curtailment mitigation techniques, air conditioner use has been identified as one source to help control electricity demand by using demand response techniques and human behavioural management. As part of this, primary data regarding the use of aircon is currently being observed in several rooms across Hiroshima University but mostly in the IDEC department second floor where most the classroom are located. This data is currently air conditioner set temperature, adjusted temperature, actual air temperature/humidity. Currently this data is being sampled semi-randomly but hopefully, soon some automatic sensors can be installed to measure the actual temperature/humidity within the most commonly used rooms.

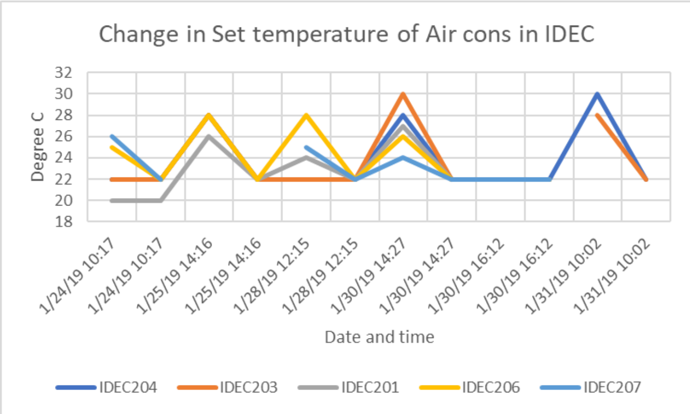

Figure 20: Change in set temperature of Aircons in IDEC

Lastly, as part of the behavioral analysis a survey will be created and sent out to students in Hiroshima University to understand the current knowledge and behavior towards air conditioners to better understand the use of air conditioners and thereafter some strategies can be designed to change this air conditioner use to better suit the environment and the electricity company and thus hopefully reducing curtailment.

3.2 Methodology

Currently, the methodology is not fully established yet, the flow diagram below shows the basic idea although more work needs to be done in how to estimate the future curtailment. Monte Carlo simulation is one possible solution. One literature review that is currently taking place is about using Monte Carlo method to simulate energy markets. (Amelin, 2004)

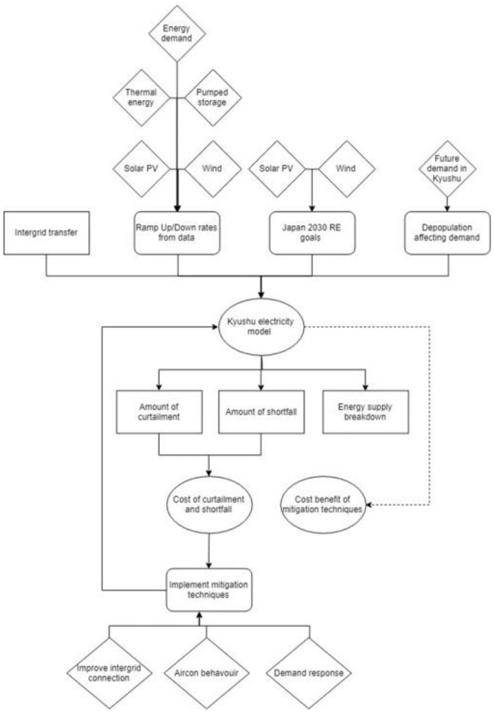

Figure 21: Simulation flow chart(preliminary)

4. Results

As stated, there are no results yet to discuss since most time has been spent on background, data collection and initial analysis. However, the graph below shows the first ever curtailment in Japan that occurred in Kyushu and this may help in understanding the conditions that occurred just before, during and after the curtailment which can be used to understand why the curtailment occurred and what may be done to reduce it in the future.

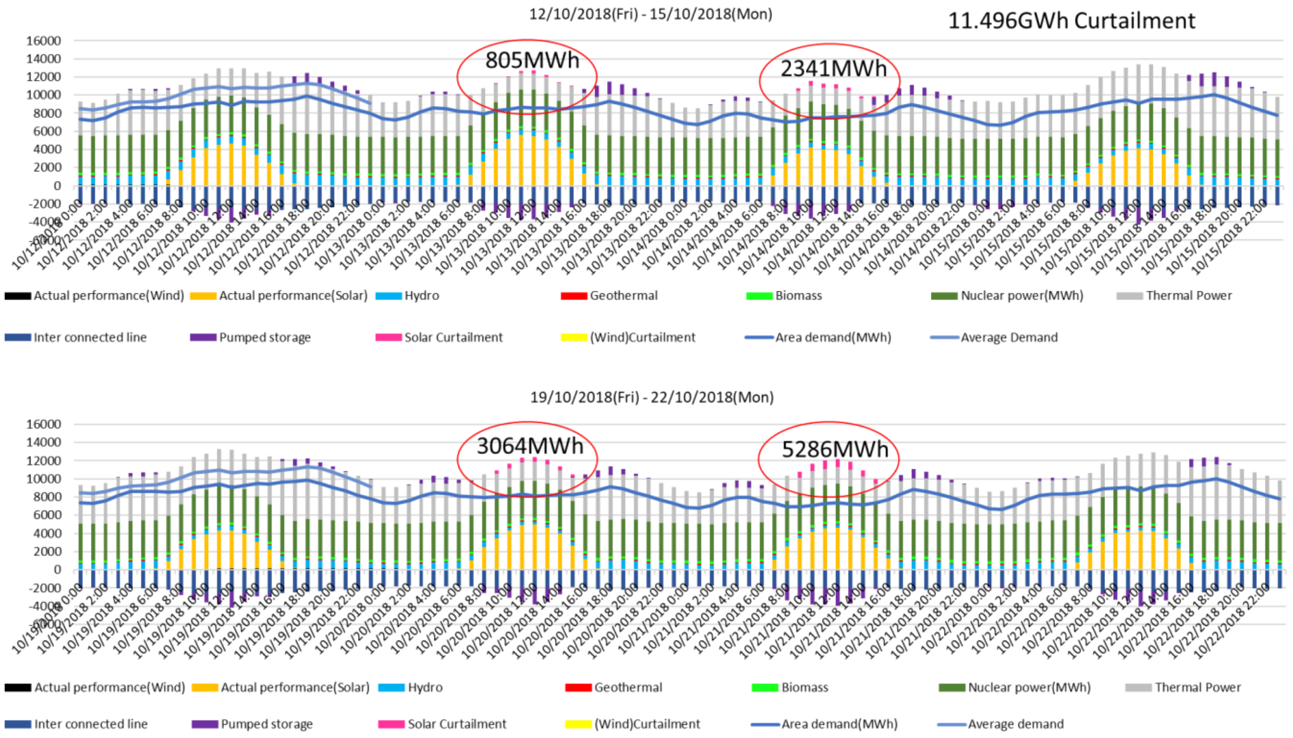

Figure 22: Two weekends in 2018 which experienced RE curtailment in Kyushu

The graphs above show one day before curtailment, the days that curtailment occurred and then the day after curtailment to try understanding if there are any relationships between the energy management before during and after curtailment. The first thing to notice is the average demand curve which shows the average demand for the 2018 at each time interval. Immediately its clear that these days all experienced demand lower than the average demand. This makes sense since this curtailment occurred during October which is during the autumn season in Japan. As the solar PV increases from about 8 am its clear that the thermal energy(grey) absorbs most of the increased energy by lowering its output. However, there is a limit to how much can be reduced, and this is the ramp up/ ramp down time, which will be used in calculating the curtailment in the future, this will be discussed at a later stage. Its clear that at the same time as the increase in PV there is also a negative amount of pumped storage consumed, this is absorbing some of the increased energy by moving water, storing this energy for later use. The inter grid connection also increases, however it is limited by the low capacity between Kyushu and Chugoku regions. Curiously, the amount of energy absorbed by the pumped storage is a) not the maximum amount of pumper storage available and b) only a small percentage of the storage energy is released after the solar PV is generated, leading to the question, how is the pumped storage controlled, and what are the limiting factors to its use. Both of these questions will be posed to Kyushu electric during a yet to be planned meeting.

5. Things to be done further

Next step is to meet with Kyushu electric and asked them the following questions

- Find out about prediction methods, why such large disparities between predicted and actual supply for both wind and solar
- How can a more accurate estimation of RE supply help with electricity management
- Why not full use of pumped storage?
- Why such low pumped storage efficiency? 53% vs 80% worldwide average
- As RE increases in Kyushu, what will be the impact on energy management?
- Demand management techniques implemented?
- Get supply distribution for thermal (Coal, oil, gas)
- Use of Inter grid connection, and reserve margin
- Why the sudden increase in biomass between Q2 and Q3 2018? Looks to me like a data error

Thereafter, using the existing calculated ramp up and ramp down rates for Solar PV, wind, thermal energy and pumped storage calculated from the existing data, increase the percentage of solar and wind in line with the 2030 goals and see how curtailment is affected. Then work out the total value of this curtailment up until 2030 with no mitigation methods implemented.

At the same time, develop one survey to determine the current behaviour of students towards air conditioner use. Also test existing air conditioners in IDEC, by using several temperature sensors placed around the room and outside and measure how long the air conditioner takes to reach the set temperature. Then ask students to enter and give them a short survey asking about what they perceive the temperature to be and how comfortable they think it is.

Later, develop a demand response unit for air conditioners that allow time of day tariffs to be implemented retroactively without the large infrastructure requirements of the traditional, whole house, time of day metering.

Lastly, calculate how much energy the behavioural modification and demand response unit may save and then apply this to the original model to calculate how much electricity can be saved, how much curtailment can be avoided and the total money saved. Then make recommendations about which mitigation method has the best cost to benefit.

References

Amelin, M. (2004). *On Monte Carlo Simulation and Analysis of Electricity Markets*.

Bird, L., Lew, D., Milligan, M., Carlini, E. M., Estanqueiro, A., Flynn, D., … Miller, J. (2016). Wind and solar energy curtailment: A review of international experience. *Renewable and Sustainable Energy Reviews*, *65*, 577–586. https://doi.org/10.1016/j.rser.2016.06.082

Kimura, K. (2017). Feed-in Tariffs in Japan: Five Years of Achievements and Future Challenges, (September), 1–22. Retrieved from https://www.renewable-ei.org/en/activities/reports/img/pdf/20170810/REI_Report_20170908_FIT5years_Web_EN.pdf

SHINKAWA, T. (2018). Electricity System and Market in Japan, (January).

Trevor M. Letcher. (2016). Storing Energy: with Special Reference to Renewable Energy Sources.

Kyushu Electric. (2019, January 20). Overview of consignment supply etc. Retrieved from Kyushu Electric:

http://www.kyuden.co.jp/wheeling_liberal.html

Kyushu Electric. (2019, January 20). Publish lineage information. Retrieved from Kyushu Electric: http://www.kyuden.co.jp/wheeling_disclosure.html

[CHESS Lab semester summary seminar handout]

Simulation and Management of Photovoltaic Power Supply in Northern KZN with Smart Metering

Mbalenhle Shabalala

Graduate School for International Development and Cooperation (IDEC), Hiroshima University, Japan.
Electrical Engineer, KZN OU, Distribution, ESKOM Holdings SOC Ltd.

1. Abstract

South Africa (RSA), like the rest of the world has seen an increase in electricity supply demand mainly due to new electrification. In Northern KwaZulu Natal (a largely rural part of the province of RSA), it has led to the current Sub Transmission and Distribution infrastructure's inability to supply the demand. This area is supplied by two transmission substations, Normandie Substation (400 kV/ 132 kV) and Impala Substation (275 kV/ 132 kV) supplying 13 distribution substations. The study area was chosen because of the load growth that has resulted in violation of thermal loading as per the NSR048 Grid code stipulations(Bello, M. *et al.*, *2014*) .The grid code stipulates that the HV busbar voltages should remain *0.95 p.u.* and above under normal operating conditions(Bello, M. *et al.*, *2014*). The challenges faced by Eskom, (Eskom Holding SOC Ltd is a South African power utility company responsible for approximately 91% of the country's power supply), in planning for additional capacity for the area; are the vast environmental constraints such as wetlands, large commercial farms, game reserves and the required large capital contributions.

The research aims to address these issues by exploring alternative renewable energy sources, such as PV to provide the required supply through distributed energy generation simulations. The study will be evaluating the hosting capacity of distribution medium voltage feeders (MV feeders, 33kV-11kV), as well as at substation level through simulations. "PV hosting capacity" is the maximum PV penetration, at which no technical constraints are violated(Ismael *et al.*, 2019). The research will explore opportunities and challenges DEG integration will bring such as power quality issues, co-ordination of DEG and centralized generation, battery energy storage, smart invertors, DER Management Systems (DERMS) and possible effects on the HV system fault levels. The strategic positioning of the PV plant will consider the solar irradiance of the area, the required capacity, the integrated distribution feeder hosting capacity, (integration before strengthening of the distribution network is required) the type of customer in the area and cost benefit analysis.

2. Introduction

2.1. Background on Current South African Energy Sector

Electricity in South Africa is supplied by Eskom Holdings SOC Ltd (ESKOM), a public utility responsible for 91% of the entire country's electricity supply; the rest is supplied by the Municipalities (1.77%) and Independent Power Producers (IPPs) supply the remaining 7.21% [9]. RSA is also part of South African Power Pool (SAPP), trading electricity with neighboring countries, viz. Botswana, Lesotho, Mozambique, Namibia, Swaziland, Zambia, and Zimbabwe. A total of 9,703 GWh was imported in 2015/2016 with exports of 13,465 GWh in the same period [9]. The transmission line voltages range from 765 kV to 132kV and 533 kV line DC monopolar going to Mozambique. Distribution lines voltages range from 88 kV to 11 kV.

2.2. Study Area

The Normandie and Impala Main Transmission Stations (MTS) are connected to long radial 132kV lines supplying 13 distribution substations with a normally open HV breaker situated at Mkuze Substation. Due to long distribution lines, the distribution substations on these lines presently experience low HV busbar voltages and Impala-Nseleni line is experiencing high thermal loading of over 80% [Figure 1]. Both these operating scenarios are in direct violation of the of Grid code. This is largely influenced by the growing number of illegal connections onto the networks over the years. The current household electrification backlog for the area supplied by Impala-Normandie MTS is approximately 300 000 connections.

This supply area is largely rural and the backlog is due to investment neglect the area faced under the previous apartheid government administration. Any capacity planning since then has been hindered by budget constraints and the protected environmental areas. The area has an immense number of game reserves, wetlands, forest reserves and it is a hub for commercial farming such as maize, sugar cane and various fruits.

This area experiences a constant load profile throughout the year, i.e. the transformer loads do not have a fluctuating winter peak load and summer peak load. This translates to consistently low HV busbar voltages throughout the year. Figure 1 shows the population density of KwaZulu Natal.

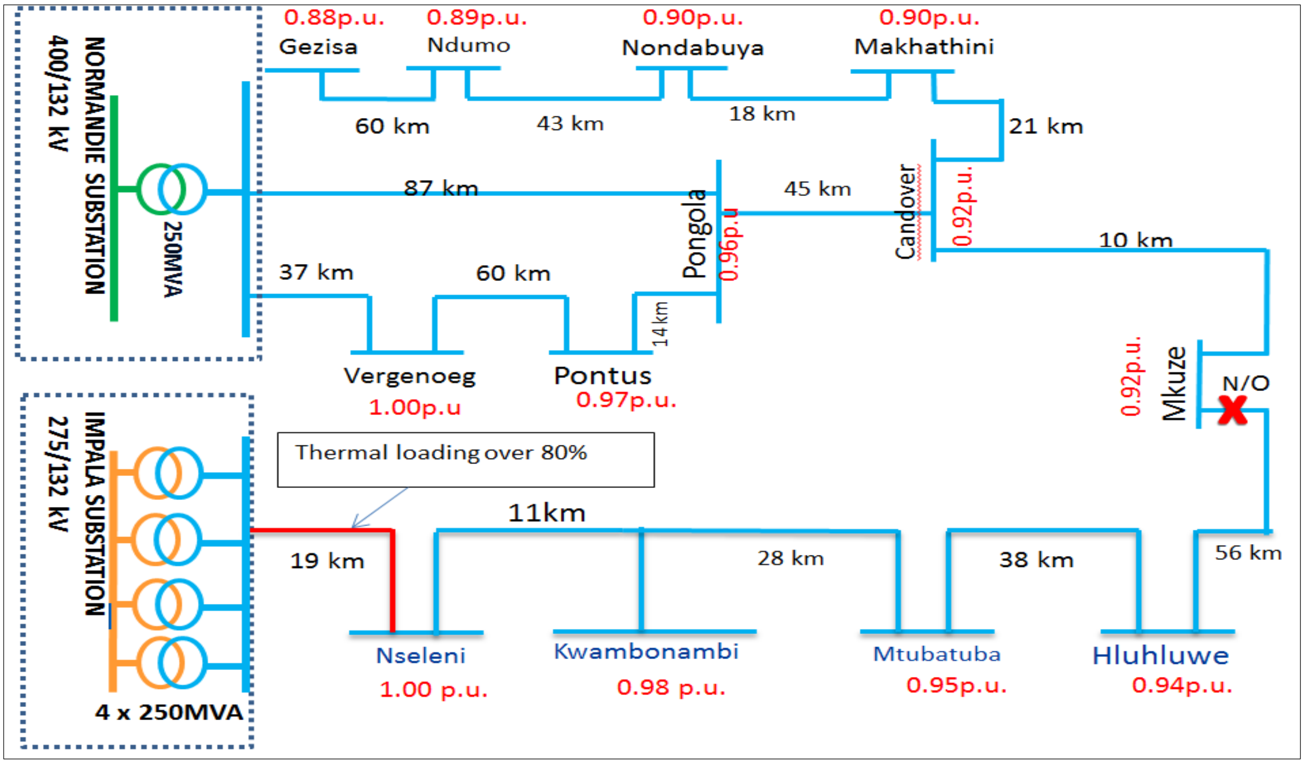

Figure 23: Single line diagram of the of the sub-transmission network

[CHESS Lab semester summary seminar handout]

3. Literature Reviews

3.1. Title

J. S. Thomas, J. John, N. Saji, N. M. Sunny, A. Krishnan and T. Mathew, "Design And Financial Analysis Of A Micro Grid-Tie Solar PV System For A Small Scale Industry In Kerala"

Objectives

The paper explores the feasibility of a Micro Grid-Tie Solar PV System by setting up a grid-tied solar inverter system in a carefully chosen small-scale industry which can use the solar PV power plant to deliver power required by the base load of the plant. It also employs the advantage of using solar PV systems which promote sustainable development with fewer burdens on the environment. A small-scale industry farm, Kurishumala Dairy Farm, Vagamon, that produces packet milk was selected as the case study

Data and methodology

The data used to for the paper was solar radiation ranges from 4-7 kWh/ m^2 per day. The site is located top of a hill at Latitude-9.6°N and Longitude-76.9°E. The ambient temperature range at the site is between 10°C and 23°C. The site consumes an average energy of 71 kWh per day. The minimum peak sun hours is taken as 4 hours for 200 days in a year. This means that at least 4 kWh per day is available from a 1kWp solar PV plant. Tilt Angle of Solar Panels is chosen as 20 degrees. The total connected load of the industry is 461kW. The collected data was used to ccalculate, Load to be supplied by PV system, inverter Rating, PV Array Sizing and the maximum output power. The temperature coefficient and ambient temperature was assumed.

Main findings

A simple design approach for proposing a micro grid-tied battery-less solar PV system for a small scale industry was found to be feasible. Investment return of 10 years is too slow as the equipment is close to reaching its life span of 15 years.

Relationship to my research and Things to be improved

The paper conducts explicit calculations for the notified maximum demand (NMD) VS actual consumption of the case study and designed a solar plant to meet the NMD which my research requires as well. It however does not consider the effects of the tying the system to the grid has on power quality and how the customer can switch between the two systems or state if it is not possible and the PV can only work as a standalone unit. Assumptions could be reduced or improved by choosing and existing PV module and use actual manufacture specifications for more accurate results.

3.2. Title

Ian Vincent Poole and Frank Dinter, *"A Molten Salt Tower Model used for Site Selection in South Africa using SAURAN Meteorological Data"*, Solar Thermal Energy Research Group, Stellenbosch University, Stellenbosch, South Africa

Objectives

The paper investigates South Africa's potential for concentrating solar power (CSP) while taking into account the two main limitations for CSP plants i.e. electrical transmission and water availability.

Data and Methodology

The site used satellite data derived DNI information from European Community Solar Data (SoDa) datasets was available for all six of the sites with an hourly resolution (12 years), ground measured, 1 minute resolution DNI data is available from the South African Universities Radiation Network (SAURAN) (1 year because the station is new), historical wind and temperature data from weather stations near to the sites, courtesy of the South African Weather Service (10 years) and measured wind speed. The case study simulated six different sites using MATLAB® Simulink for a 100 MWe molten salt tower plant and compared results. The plant included 12 hours of storage

Main findings and relation to my research

Even though Laingsburg has the third highest electrical yield, when transmission and water resource availability is factored in, it is the optimal choice for the CPS plant in terms of operation costs. It also emphasizes the importance of grading the properties of each calculation to for sound financial investments.

Things to be improved

Therefore it did not consider the optimization of solar field area, receiver size, or thermal storage volume.

3.3. Title

Hamdy M. Sultan, Oleg N. Kuznetsov, Ahmed A. Zaki Diab, "*Site Selection of Large-Scale Grid-Connected Solar PV System in Egypt*",. Department of Electrical Power Systems, Moscow Power Engineering Institute "MPEI" Moscow, Russia, Electrical Engineering Department, Faculty of Engineering, Minia University Minia, Egypt.

Objectives

This study explored the potential of large-scale grid connected solar PV generation in Egypt in order to present a technical, economic and environmental investigation of implementing PV power plants of 100 MW capacity at selected promising sites in Egypt.

Data and Methodology

The paper used DNI data ranging from 2000-3200 kWh/m^2/year, the minimum solar radiation range from 5.38 kWh/m^2/day to 6.64 kWh/m^2 /day , the daily sunshine duration hours range between 9-11 hours/day and the manufacturer specifications of the 200 W peak Sanyo mono-Si-HIP-200BA3 PV-module. 27 locations were assessed for their technical potential considering a 100 MW PV power plant at each site.

The project viability analysis was accomplished based on RETScreen Expert package simulation depending on electricity production, financial, and CO2 emission analyses. Considering the distance between the selected site and grid integration point, described by transmission lines and substations and factored in climate, water resources, electrical and Transport Networks, land-use and availability of vacant land.

Main findings

The maximum energy yield of 299.205kWh/m^2 was produced at Kossier while the lowest value of 261.53kWh/m^2 was at Cairo airport. The overall average specific energy yield has been 279.616kWh/m^2. The maximum annual energy generation of 176.53 GWh was obtained from Kossier, and at least 154.30 GWh of a power plant near Cairo airport. For this simulation, the highest yield was also the closest to transmission lines and highways and other environmental factors.

Things to be improved

It did not consider peak sunshine hours; it assumed the solar radiation was at its maximum the entire 12 hours of sunshine.

4. Objectives

The objective of this research project is to study how solar photovoltaic (PV) plant models can be used to provide additional capacity by focusing on the ideal site selection for PV plants through PV integration analysis and addressing the arising effects it generates on the power grid.

- The first step would be performing load forecast simulations using PowerGLF to model the required additional capacity considering summer and winter peak loads for assessment.
- Collect climate data, viz. solar radiation, ambient temperature, wind speed and altitude to calculate the total output power that can be generated from a PV array at any given location (The design point direct normal irradiance (DNI) will be selected as 1000 W/m^2 at peak sunshine hours for all of the simulations, due to the profuse levels of DNI available in South Africa).

1.1. PV Hosting Capacity Simulations

- Choose a single MV network from each of the 13 distribution substations in this case study to conduct load flow simulation studies to determine the hosting capacity of each network.
- Using MatLab/Simulink software and DigSilent (PowerFactory), model the PV plant and simulate with a bidirectional inverter to compensate for the voltage rise through reactive power control (Watson *et al.*, 2016).
- Conduct "Do Nothing Scenario" DEG hosting capacity simulations, monitoring system stability for operational limit violations viz. under and overvoltage, thermal overloading, power quality and protection.
- The next phase will attempt to increase the hosting capacity of each network using HC enhancement techniques such as battery storage, active power curtailment, harmonics control, network reconfiguration, reactive power control and On-Load-Tap-Changer (OLTC) transformers.
- Identify the most favourable site for future integration of DEG based on electrical yield and cost of

generating electricity of at the site.

1.2. Smart grid

The smart grid is the recent electric power grid infrastructure for improved efficiency, reliability and safety, with smooth integration of renewable and alternative energy sources, through automated control and modern communications technologies(Jain *et al.*, 2014). Considering the study area is largely rural, Power Line Communications (PLC) present the best advantage for a smart meter. PLC is a suitable and advantageous telecommunication solution for utilities engaged with smart grid deployments since both MV and LV grids can be used to host a telecommunications network capable of providing a future proof communications network for smart metering and smart grid deployments(Sendin *et al.*, 2014) . This kind of metering is currently not used by Eskom.

5. Data and methodology

5.1. Data

Conducting load flow analysis on MV distribution networks requires measurement of the actual load on the network. These measurements can be downloaded from statistical metering units on the SCADA system. The table below shows the sample of the format the data comes in. The South African weather service provided climate data comprising of temperature, rain, wind speed, and elevation above sea level.

Table 3: statistical metering data

DATE	TIME	YEAR	MONTH	DateNo	Day of Week	KW	KVAR	LEKSAND NB1	PF
2015/01/01	00:00	2015	January	1	Thursday	1960	708	2083.95	0.941
2015/01/01	00:30	2015	January	1	Thursday	1944	696	2064.84	0.941

3.2 Methodology

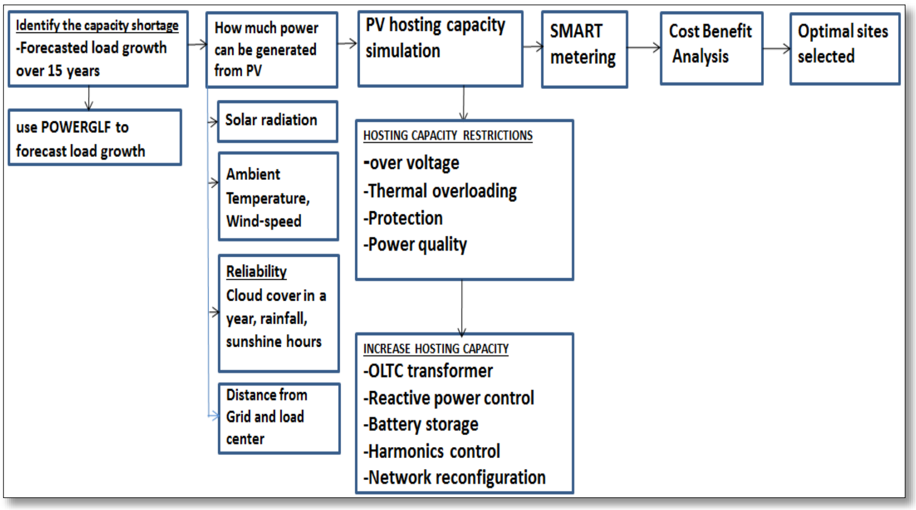

Figure 24: methodology flowchart

6. Describe the methodology for data analysis.

Statistical metering is used for both load forecasting and load flow simulations. Data gathering is the most important aspect supporting an accurate load forecast. Because of the nature of load forecasting no minimum or maximum dataset can be specified – irrespective of the amount of data available a forecast can and should be produced. Data range from billing history, location data, development plans, existing networks etc. The amount of data available will influence the accuracy of the forecast. Data required for a load forecast comprise attribute data, as well as geographical data. Using statistical metering the load profile of the network is populated into power factor to calculate end voltage and thermal loading.

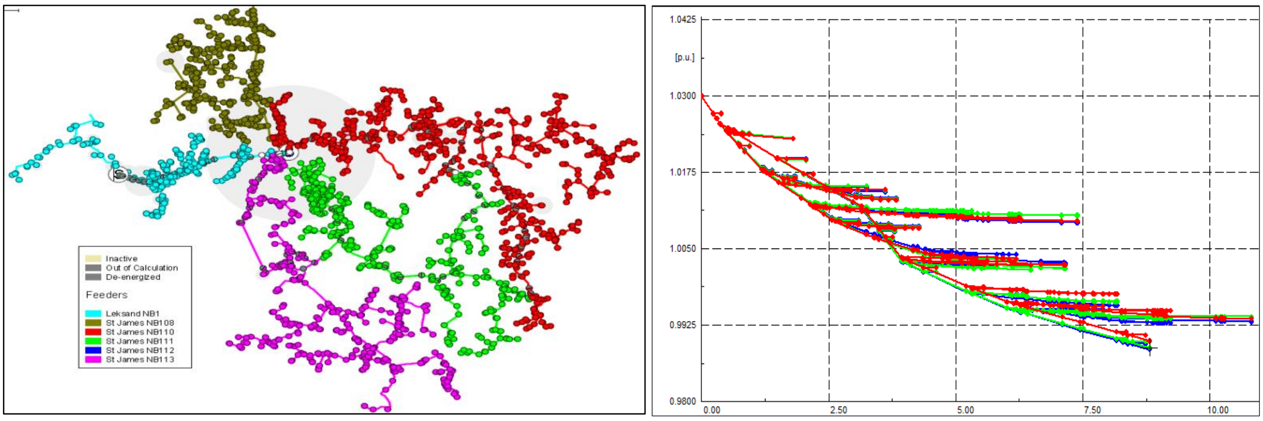

Figure 25: Network layout on PowerFactory and the resulting voltage profile

At this stage the resulting load flow results will be used to select and reduce the networks for the case study form 52 to 12 networks. This is achieved by using EPRI's Distribution Resource Integration and Value Estimation (DRIVE) tool. MV PF casefiles are analyzed by Drive MBI, the output feeds into the DRIVE Tool and DRIVE assesses hosting capacity and delivers interactive results. Below is a table of data that feeds into DRIVE and Figure 4 shows two presentations of results that are produced at the end.

Table 4: Resulting Node Data Exported From PowerFactory

NodeID	VANpu_peak	VBNpu_peak	VCNpu_peak	ThrukWA_peak	ThrukWB_peak	ThrukWC_peak	Thrukvar A_peak	Thrukvar B_peak	Thrukvar C_peak	LoadingA_peak	LoadingB_peak	LoadingC_peak
'PointTerm3358'	1.03	1.03	1.03	491.2956	491.1044	491.2143	106.4961	106.4797	106.3224	0.006148	0.006146	0.006147
'PointTerm3361'	1.03	1.03	1.03	491.2956	491.1044	491.2143	106.4962	106.4797	106.3224	0.007685	0.007682	0.007683
'PointTerm3364'	1.03	1.03	1.03	491.2956	491.1044	491.2143	106.4962	106.4797	106.3224	0.003843	0.003841	0.003842

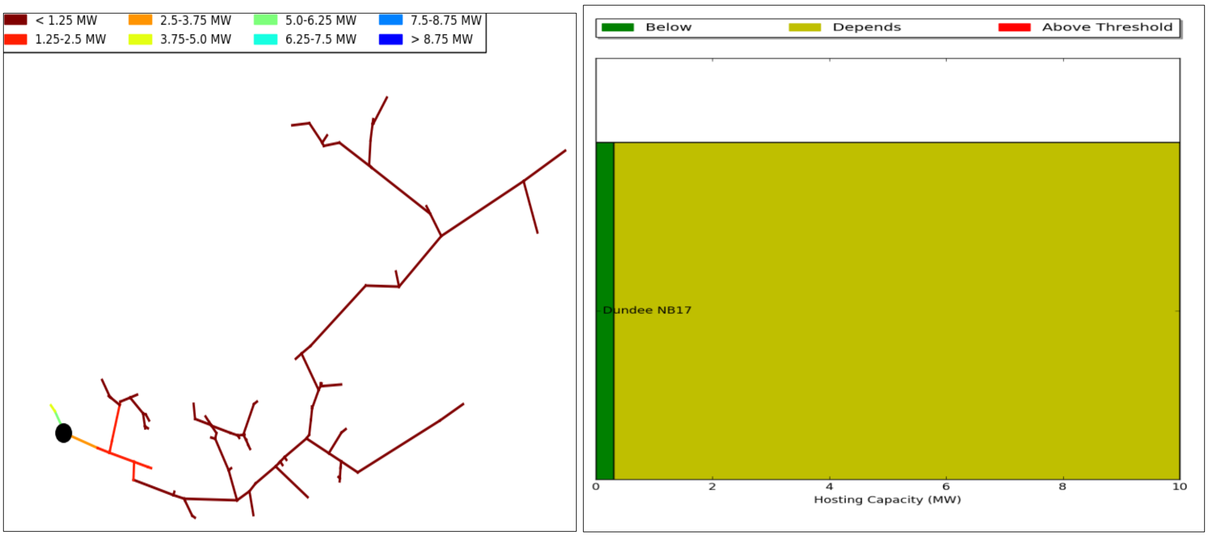

Figure 26: Drive tool results representation

7. Results

The Drive tools proved helpful for filtering the networks but more reading and understanding has to be done.

8. Discussion and Limitation

Obtaining primary data proved challenging for the case study as some data sources proved incomplete data or does not have readily available on the internet and requires a human factor to obtain which affects turn-around time. Processing some raw data and operating new software or learning new functions of already in use software is an area that requires further attention and optimization.

9. Things to be done further

- The acquired climate data from RSA weather service has to be processed; further climate data such solar radiance measurements still needs to be collected and sunshine hours assumed since this data is not measured.
- Run load flow simulations for all the remaining networks
- Conduct further load forecasting and finish choosing the case study networks
- Choose PV Module for a more accurate calculation.
- Identify a suitable costing method for financial calculation that provides the best project evaluation model for optimal investment return.
- Further literature study related to subject.

10. References

1. Bello, M. *et al. (2014)* 'DST_34-542: Distribution Voltage Regulation and Apportionment Limits Standard', Planning and GIS, Eskom Hld SOC LTD.
2. Ismael, S. M. *et al.* (2018) 'State-of-the-art of hosting capacity in modern power systems with distributed generation', *Renewable Energy*. Elsevier Ltd, 130, pp. 1002–1020. doi: 10.1016/j.renene.2018.07.008.
3. Watson, F. *et al.* (2016) 'Integrated systems testing of a smart home for increased grid hosting capacity', *IEEE Power and Energy Society General Meeting*, 2016–November, p. 7741989. doi: 10.1109/PESGM.2016.7741989.
4. Jain, S. *et al.* (2014) 'Survey on smart grid technologies-smart metering, IoT and EMS', *2014 IEEE Students' Conference on Electrical, Electronics and Computer Science, SCEECS 2014*, p. 6804465. doi: 10.1109/SCEECS.2014.6804465.
5. Sendin, A. *et al.* (2014) 'PLC deployment and architecture for smart grid applications in Iberdrola', *IEEE ISPLC 2014 - 18th IEEE International Symposium on Power Line Communications and Its Applications*, (June 2013), pp. 173–178. doi: 10.1109/ISPLC.2014.6812374.

[CHESS Lab semester summary seminar handout]

SOCIAL MEDIA FOR DISASTER DAMAGE ASSESSMENT

Wirawan Widiyanto[1]

[1]CHESS Lab, Department of Development Technology,
Graduate School of International Development and Cooperation, Hiroshima University

1. Introduction

Disaster risk is strongly connected to the processes of human development. Disasters put development at risk but also at the same time, the development choices made by individuals, communities or nations can generate new disaster risk. On the other hand, human development can also contribute to the reduction of disaster risk (UNDP, 2004) that provide opportunities for physical, social, political and environmental development that may not have been available before the disaster (Hayat & Amaratunga, 2017). Disaster management is all activities involving organization, planning and application of measures preparing for, responding to and recovering from disasters (United Nations, 2016). In disaster management, several abilities is needed namely: the ability to determine the harshness of disaster by population and location; and the ability to communicate early warning for all population especially that in the risk area (Carley, Malik, Landwehr, Pfeffer, & Kowalchuck, 2016). Nowadays, information gathered for disaster management comes from field survey, traffic camera, satellite and aerial images (Eilander, Trambauer, Wagemaker, & Van Loenen, 2016).

Unlike other traditional ways, social media platform can obtain large scale of data and information (Wu & Cui, 2018). Big data analysis, that comes from social media data, can help the authorities to obtained the right information therefore can made best action as possible (Ragini, Anand, & Bhaskar, 2018). Twitter as one of the most popular social media platforms use in this study because Twitter can be seen as important media for communication in disaster management because its coverage and data collection (Carley et al., 2016). Twitter also has an Application Programming Interface (API) to facilitate developers and researchers to study Twitter data by submitting text-based queries in pre-specified formats to Twitter and Twitter will return text-only data (Carley et al., 2016). Although data obtained from Twitter can bring big contribution in disaster management, but it is important to explore if there is correlation between data derived from Twitter and actual field conditions (Wu & Cui, 2018).

2. Objectives

The objective of this study is to:

- Simulate the affected area by using Twitter data.
  I would like to simulate disaster map by using information that was obtained from Twitter Streaming API regarding people report on the current condition of the effected area after Sunda Strait Tsunami happened.
- Determine the actual affected area.
  I would like to generate disaster map from damage and lost assessment report from the government and others report from research that was conducted in the effected area. This disaster map will be use to examine the

effectiveness of the simulated disaster map from Twitter data.

3. Data and methodology

3.1 Data

For the first objective, this study will be using text data with JavaScript Object Notation (JSON) format that collected from Twitter Streaming API. While for the second objective will be using location data from government damage assessment report on Sunda Strait Tsunami and others research report that was conducted in the effected area of Sunda Strait Tsunami.

3.2 Methodology

Data analysis focused on how to categorized the text data obtained from Twitter Streaming API in order to selecting the Tweets that generated from effected area that reporting on the current condition regarding the victims and infrastructure condition after the Sunda Strait Tsunami.

4. Discussion and Limitation

For this study progress, I have started the collection data process by making the developer account on Twitter. With this account, I can create a Twitter App to generate access token, access token secret, consumer key and consumer secret that will be needed in the Python script in order to connect to the Twitter Streaming API therefore the data can be downloaded.

5. Things to be done further

I would like to continue on data collecting with the help of learning on Python and one of the Python library Tweepy. Also, I will start to collect government report on disaster damage and lost assessment in Banten and Lampung. I will also need to read more previous study especially on Twitter data mining to more understanding regarding the method in order to improve this study methodology.

References

Carley, K. M., Malik, M., Landwehr, P. M., Pfeffer, J., & Kowalchuck, M. (2016). Crowd sourcing disaster management: The complex nature of Twitter usage in Padang Indonesia. *Safety Science*, *90*, 48–61. https://doi.org/10.1016/j.ssci.2016.04.002

Eilander, D., Trambauer, P., Wagemaker, J., & Van Loenen, A. (2016). Harvesting Social Media for Generation of Near Real-time Flood Maps. *Procedia Engineering*, *154*(0), 176–183. https://doi.org/10.1016/j.proeng.2016.07.441

Hayat, E., & Amaratunga, D. (2017). The Role of Local Government in Post-Disaster Road Reconstruction: Assessment of Factors Affecting Local Government Road Maintenance Capacity. In R. Djalante, M. Garschagen, F. Thomalla, & R. Shaw (Eds.), *Disaster Risk Reduction in Indonesia - Progress, Challenges, and Issues* (p. 255). Springer International Publishing AG 2017. https://doi.org/10.1007/978-3-319-54466-3_10

Ragini, J. R., Anand, P. M. R., & Bhaskar, V. (2018). Big data analytics for disaster response and recovery through sentiment analysis. *International Journal of Information Management*, *42*(May), 13–24.

https://doi.org/10.1016/j.ijinfomgt.2018.05.004

UNDP. (2004). *Reducing Disaster Risk: a challenge for development*. (M. Pelling, A. Maskrey, P. Ruiz, & L. Hall, Eds.). New York: John S. Swift Co., USA.

United Nations, U. (2016). *Report of the open-ended intergovernmental expert working group on indicators and terminology relating to disaster risk reduction* (Vol. 21184).

Wu, D., & Cui, Y. (2018). Disaster early warning and damage assessment analysis using social media data and geo-location information. *Decision Support Systems*, *111*(October 2017), 48–59. https://doi.org/10.1016/j.dss.2018.04.005

https://marcobonzanini.com/2015/03/02/mining-twitter-data-with-python-part-1/

http://adilmoujahid.com/posts/2014/07/twitter-analytics/